AD_____

Award Number: DAMD17-98-1-8171

TITLE: Epidermal Growth Factor Receptor Overexpression as a Target for Auger Electron Radiotherapy of Breast Cancer

PRINCIPAL INVESTIGATOR: Raymond Reilly, Ph.D.

CONTRACTING ORGANIZATION: The Toronto Hospital
Toronto, Ontario M5G 2C4 Canada

REPORT DATE: August 2000

TYPE OF REPORT: Annual

PREPARED FOR: U.S. Army Medical Research and Materiel Command
Fort Detrick, Maryland 21702-5012

REPORT DOCUMENTATION PAGE

OMB No. 074-0188

1. AGENCY USE ONLY (Leave blank)	2. REPORT DATE	3. REPORT TYPE AND DATES COVERED
	August 2000	Annual (1 Jul 99 - 1 Jul 00)

4. TITLE AND SUBTITLE
Epidermal Growth Factor Receptor Overexpression as a Target for Auger Electron Radiotherapy of Breast Cancer

5. FUNDING NUMBERS
DAMD17-98-1-8171

6. AUTHOR(S)
Raymond Reilly, Ph.D.

7. PERFORMING ORGANIZATION NAME(S) AND ADDRESS(ES)
Toronto General Hospital
Toronto, Ontario M5G 2C4 Canada

E-MAIL: raymond.reilly@utoronto.ca

8. PERFORMING ORGANIZATION REPORT NUMBER

9. SPONSORING / MONITORING AGENCY NAME(S) AND ADDRESS(ES)
U.S. Army Medical Research and Materiel Command
Fort Detrick, Maryland 21702-5012

10. SPONSORING / MONITORING AGENCY REPORT NUMBER

11. SUPPLEMENTARY NOTES
Report contains color photos

12a. DISTRIBUTION / AVAILABILITY STATEMENT
Approved for public release; distribution unlimited

12b. DISTRIBUTION CODE

13. ABSTRACT *(Maximum 200 Words)*

The epidermal growth factor receptor (EGFR) is overexpressed in the majority of estrogen receptor-negative, hormone-resistant and poor prognosis breast cancers. Our objective is to evaluate a new form of targeted radiotherapy for EGFR-positive breast cancer. Our approach is to exploit the normal internalization and nuclear translocation of human EGF following binding to the EGFR to introduce the Auger electron-emitting radionuclide, indium-111 (^{111}In) into breast cancer cells, where the Auger electrons are damaging to DNA causing cell death. We constructed a novel human serum albumin-human EGF bioconjugate (HSA-hEGF) substituted with multiple DTPA metal chelators for ^{111}In for targeted Auger electron radiotherapy of breast cancer. ^{111}In-DTPA-HSA-hEGF was specifically bound by EGFR-positive MDA-MB-468 human breast cancer cells and was internalized and translocated to the cell nucleus. ^{111}In-DTPA-HSA-hEGF was radiotoxic to MDA-MB-468 cells *in vitro* and localized effectively in MDA-MB-468 breast cancer xenografts *in vivo* achieving a tumour/blood ratio of >7:1 at 72 hours post-injection. Concurrent studies demonstrated that ^{111}In-DTPA-hEGF was 30 to 500-fold more cytotoxic *in vitro* (on a molar basis) than conventional chemotheraputic agents used to treat breast cancer. Studies are planned to evaluate the efficacy and toxicity of targeted Auger electron radiotherapy of MDA-MB-468 breast cancer xenografts *in vivo*.

14. SUBJECT TERMS	15. NUMBER OF PAGES
Breast Cancer, Auger electrons, indium-111, EGFR, EGF	43
	16. PRICE CODE

17. SECURITY CLASSIFICATION OF REPORT	18. SECURITY CLASSIFICATION OF THIS PAGE	19. SECURITY CLASSIFICATION OF ABSTRACT	20. LIMITATION OF ABSTRACT
Unclassified	Unclassified	Unclassified	Unlimited

FOREWORD

Opinions, interpretations, conclusions and recommendations are those of the author and are not necessarily endorsed by the U.S. Army.

___ Where copyrighted material is quoted, permission has been obtained to use such material.

___ Where material from documents designated for limited distribution is quoted, permission has been obtained to use the material.

___ Citations of commercial organizations and trade names in this report do not constitute an official Department of Army endorsement or approval of the products or services of these organizations.

X In conducting research using animals, the investigator(s) adhered to the "Guide for the Care and Use of Laboratory Animals," prepared by the Committee on Care and use of Laboratory Animals of the Institute of Laboratory Resources, national Research Council (NIH Publication No. 86-23, Revised 1985).

X For the protection of human subjects, the investigator(s) adhered to policies of applicable Federal Law 45 CFR 46.

N/A In conducting research utilizing recombinant DNA technology, the investigator(s) adhered to current guidelines promulgated by the National Institutes of Health.

N/A In the conduct of research utilizing recombinant DNA, the investigator(s) adhered to the NIH Guidelines for Research Involving Recombinant DNA Molecules.

N/A In the conduct of research involving hazardous organisms, the investigator(s) adhered to the CDC-NIH Guide for Biosafety in Microbiological and Biomedical Laboratories.

July 17, 2000

PI - Signature Date

TABLE OF CONTENTS

Cover 1

SF 298 2

Foreword 3

Table of Contents 4

Introduction 6

Summary of Research Accomplished in Year 1 (1998-1999) 6

Task 1: Construction, expression, purification and preliminary testing of a novel hEGF-C_H1 fusion protein 6

Research Accomplished in Year 2 (1999-2000) 7

Task 2: Construction and purification of a novel human serum albumin (HSA)-hEGF bioconjugate 7

Task 3: Radiolabelling of the HSA-hEGF bioconjugate with ^{111}In and testing for receptor binding, internalization and nuclear translocation in EGFR-overexpressing breast cancer cells. 9

Task 4: In vitro testing of relative cytotoxicity of ^{111}In-hEGF, chemotherapy and external radiation alone or in combination against EGFR$^+$ human breast cancer cells 13

Task 5: Comparison of the biodistribution and pharmacokinetics of the ^{111}In-HSA-hEGF bioconjugate and ^{111}In-hEGF in mice with human breast cancer xenografts 14

Task 6: In vitro testing of the novel ^{111}In-HSA-hEGF bioconjugate for radiotoxicity against MDA-MB-468 and MCF-7 breast cancer cell lines 17

Research Planned for Third and Fourth Year of Project 18

Completion of Current Studies

Task 4: In vitro testing of relative cytotoxicity of ^{111}In-hEGF, chemotherapy and external radiation alone or in combination against EGFR$^+$ human breast cancer cells 18

Task 6: In vitro testing of the novel ^{111}In-HSA-hEGF bioconjugate for radiotoxicity against MDA-MB-468 and MCF-7 breast cancer cell lines 19

New Studies

Task 7: Treatment of nude mice with subcutaneous MDA-MB-468 EGFR^{+} human breast cancer xenografts with ^{111}In-HSA-hEGF bioconjugate or ^{111}In-hEGF 19

Task 8: Treatment of nude mice with MDA-MB-468 human breast cancer xenografts with ^{111}In-HSA-hEGF (or ^{111}In-hEGF) and chemotherapy 19

Key Research Accomplishments **20**

Reportable Outcomes **20**

Manuscripts 20

Abstracts 21

Presentations 21

Applications for Funding Based on Research 21

Conclusions **21**

References **22**

Appendices **23**

INTRODUCTION

The epidermal growth factor receptor (EGFR) is overexpressed in the majority of estrogen receptor-negative, hormone-resistant and poor prognosis breast cancers (1). The EGFR is a transmembrane receptor tyrosine kinase which specifically binds epidermal growth factor (EGF), a 53-amino acid peptide ligand (2). Binding of EGF to the EGFR activates an intracellular signaling cascade which results in upregulation of gene expression and promotion of cell division. EGF is internalized into the cytoplasm and transported to the cell nucleus following binding to its cell surface receptor (3). We previously demonstrated that human EGF (hEGF) can act as a novel delivery vehicle to selectively introduce the Auger electron-emitting radionuclide, indium-111 (^{111}In) into the cytoplasm and nucleus of human breast cancer cells overexpressing the EGFR (4) (Appendix I). Auger electrons are very low energy electrons (<30 keV) emitted by radionuclides which decay by electron capture. Due to the extremely short, subcellular range of Auger electrons, Auger electron-emitting radiopharmaceuticals must be internalized and transported to the cell nucleus in order to exert a radiotoxic effect on cells. Once internalized however, Auger electron-emitting radiopharmaceuticals are highly damaging to chromosomal DNA and offer great potential for cancer radiotherapy (5). The restricted radiotoxicity against cells which specifically internalize the Auger electron-emitting radiopharmaceutical could potentially minimize or even eliminate the non-specific normal tissue toxicity previously observed with radiotherapeutic agents labelled with longer range β-emitters (eg. ^{131}I or ^{90}Y-labelled monoclonal antibodies) (6). We previously determined that ^{111}In-hEGF was highly and selectively radiotoxic *in vitro* to MDA-MB-468 human breast cancer cells overexpressing the EGFR (4) (Appendix I). One limitation to the use of ^{111}In-hEGF as a radiotherapeutic agent however is its rapid elimination from the blood which limits its tumour accumulation *in vivo*. Nevertheless high tumour/blood ratios (>10:1) were obtained in athymic mice implanted with EGFR-positive human breast cancer xenografts (7) (Appendix II). The overall goal of this project is to construct and evaluate a novel hEGF bioconjugate (or hEGF fusion protein) with potentially improved pharmacokinetic and tumour accumulation properties for targeted Auger electron radiotherapy of EGFR-positive human breast cancer.

SUMMARY OF RESEARCH ACCOMPLISHED IN YEAR 1 (1998-1999)

Task 1: Construction, expression, purification and preliminary testing of a novel hEGF-C_H1 fusion protein (months 1-12)

In the first year of the project (please see 1999 Annual Report for details), an expression vector was constructed for a recombinant EGF-immunoglobulin (C_H1) fusion protein containing a glutathione S-transferase (GST) affinity tag. The expression vector was under control of the $LacI^q$ promotor induced by isopropyl-β-D-thiogalactopyranoside (IPTG). E. coli were transfected with the expression vector and conditions (temperature and IPTG concentration) were optimized for expression. The expressed fusion protein was isolated from inclusion bodies under denaturing conditions (6 M guanidine or 8 M urea). The isolated fusion protein was refolded and solubilized by extensive dilution under reducing conditions (160 mM dithiothreitol) and reconcentrated to approximately 0.5 mg/mL by ultrafiltration on a Centricon-30 device. A small amount of correctly folded but sparingly soluble fusion protein was obtained that was pure, exhibited the expected molecular size for hEGF-C_H1-GST by SDS-PAGE (M_r ~18 kDa) and was

positive for EGF and GST by Western blot (Appendix III). The hEGF-C_H1-GST fusion protein bound specifically to MDA-MB-468 human breast cancer cells by flow cytometry and to isolated EGFR by ELISA. The GST affinity tag was removed by treatment with thrombin.

The amounts of sparingly soluble hEGF-C_H1 fusion protein which were obtained however were extremely small (<50-100 μg) and repeated attempts to concentrate the protein to a concentration suitable for derivatization with the metal chelator, DTPA for radiolabelling with ^{111}In (eg. 5-10 mg/mL) resulted in precipitation of the protein. It was suspected that the insolubility problem was due either to misfolding of the protein in the bacterial expression system or to exposure of hydrophobic residues in the C_H1 domain (which is coupled with the C_k domain in human IgG). Attempts to obtain a greater yield of refolded and more soluble fusion protein unfortunately were not successful.

RESEARCH ACCOMPLISHED IN YEAR 2 (1999-2000)

Task 2: Construction and purification of a novel human serum albumin (HSA)-hEGF bioconjugate (months 13-16)

Due to the limitations in obtaining sufficient quantities of soluble, concentrated hEGF-C_H1 fusion protein for further development as a radiotherapeutic agent, it was necessary to explore an alternative research strategy to achieve the objectives of the project. A decision was made to construct instead an hEGF-human serum albumin (HSA) bioconjugate which would be conceptually similar to the hEGF-C_H1 fusion protein but which would be much more soluble. The hEGF-HSA bioconjugate was constructed by reaction of maleimide-derivatized hEGF with thiolated HSA (Fig. 1).

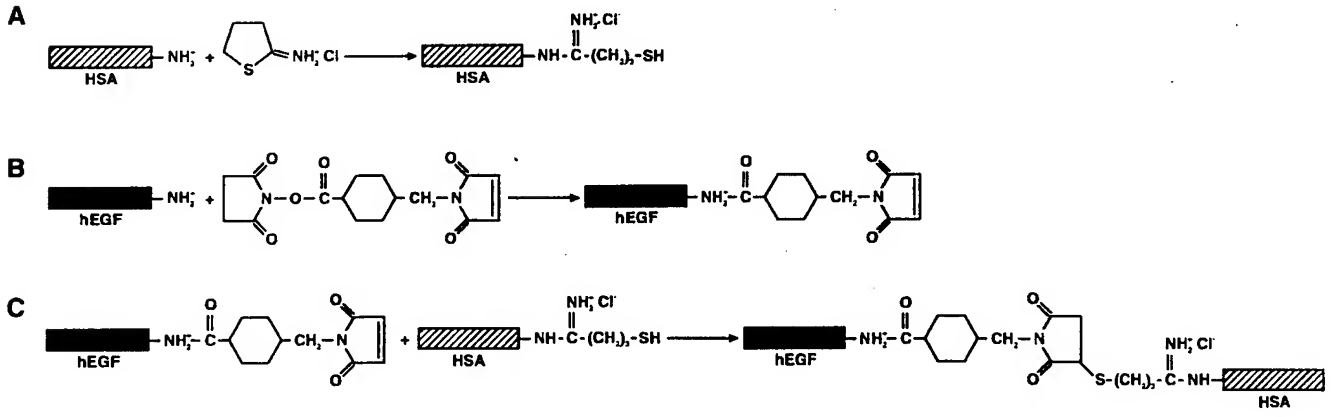

Fig. 1. Construction of hEGF-HSA bioconjugate. A. Thiol groups were introduced into HSA by reaction with Traut's reagent (2-iminothiolane). B. Maleimide groups were introduced into hEGF by reaction with sulfosuccinimidyl 4-(N-maleimidomethyl) cyclohexane-1-carboxylate (sulfo-SMCC). C. Thiolated hEGF was then reacted with maleimide-hEGF to construct the hEGF-HSA bioconjugate.

The hEGF-HSA bioconjugate was analogous to the hEGF-C_H1 protein in that it would: i) have an increased molecular size compared to hEGF (M_r 66 kDa versus 6 kDa respectively) which could potentially slow its elimination from the blood and promote tumour uptake and ii) the HSA moiety would provide multiple sites for derivatization with DTPA metal chelators for radiolabelling with ^{111}In to increase the specific activity of the radiopharmaceutical.

The monomeric hEGF-HSA bioconjugate was purified from polymeric species by ultrafiltration by passage through a Centricon YM-100 micro ultrafiltration device (M_r cut-off ~100 kDa), and from excess hEGF by passage through a Centricon YM-30 ultrafiltration device (M_r cut-off ~30 kDa). The HSA-hEGF bioconjugate was analysed for purity and homogeneity by sodium dodecylsulfonate gel electrophoresis (SDS-PAGE), Western blot and by size-exclusion HPLC. SDS-PAGE of hEGF-HSA (Fig. 2) demonstrated two major bands corresponding to proteins with M_r of ~62 kDa and ~67 kDa. Unconjugated HSA exhibited one major band with M_r of ~57 kDa and unconjugated hEGF exhibited a single band with M_r of ~6 kDa. Western blot using an anti-EGF polyclonal antibody and an anti-HSA monoclonal antibody confirmed that the bioconjugate contained both moieties (results not shown).

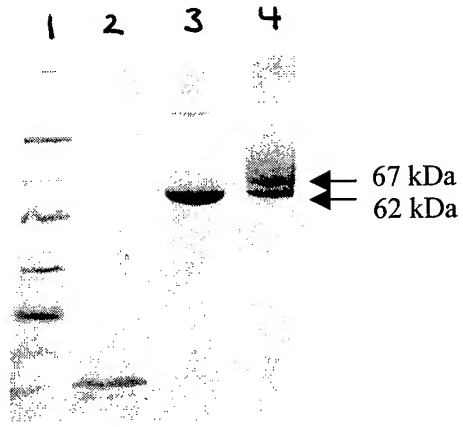

Fig. 2. SDS-PAGE of HSA-hEGF bioconjugate. Lane 1: Molecular Weight Markers. Lane 2. Unconjugated hEGF. Lane 3: Unconjugated HSA. Lane 4: HSA-hEGF.

Size-exclusion HPLC of HSA-hEGF (Fig. 3-A, p. 10) demonstrated one predominant peak with a retention time (t_R) of 11.8 minutes and a second peak with a t_R of 10.5 minutes. HPLC analysis of unconjugated HSA (Fig. 3-B) demonstrated one major peak with t_R of 10.8 minutes and a second peak with t_R of 12.1 minutes. The slightly earlier retention times for the two major peaks in the HPLC chromatogram of HSA-hEGF compared to that for unconjugated HSA sugggested only a minor increase in the molecular size of the HSA molecule when conjugated with hEGF (M_r ~6 kDa). The HPLC analysis was also consistent with an hEGF ELISA assay (ChemiKine™ Human EGF EIA kit, Chemicon International Inc., Ternecula, CA) which indicated monosubstitution of HSA with hEGF. The HPLC chromatogram for unconjugated hEGF revealed a single peak with t_R of 16.0 mins (Fig. 3-C). This peak was also visible on the HPLC chromatogram for HSA-hEGF but accounted for <2% of the total protein concentration, indicating that the HSA-hEGF bioconjugate was essentially free of unconjugated hEGF impurity.

Task 3: Radiolabelling of the HSA-hEGF bioconjugate with ^{111}In and testing for receptor binding, internalization and nuclear translocation in EGFR-overexpressing breast cancer cells (months 17-20)

HSA-hEGF was derivatized with multiple DTPA metal chelators for ^{111}In by reaction with a 10-fold, 25-fold, 50-fold or 100-fold excess of DTPA bicyclic anhydride. The conjugation efficiency was measured by trace radiolabelling an aliquot of the reaction mixture with ^{111}In acetate and determining the proportion of ^{111}In-DTPA-HSA-hEGF and ^{111}In-DTPA by instant thin layer-silica gel chromatography (ITLC-SG) developed in 100 mM sodium citrate pH 5.0. The substitution level (mols DTPA/mol HSA-hEGF) was calculated by multiplying the conjugation efficiency by the molar ratio of DTPA bicyclic anhydride:HSA-hEGF used in the reaction. These experiments demonstrated that as many as 23 DTPA molecules could be substituted onto each molecule of HSA-hEGF primarily through the HSA domain which contains 60 lysine residues for derivatization with DTPA (Table 1). Substitution of multiple DTPA groups per molecule of bioconjugate for radiolabelling with ^{111}In should significantly increase the specific activity of the radiopharmaceutical and therefore the amount of radioactivity delivered per molecule to breast cancer cells.

HSA-hEGF derivatized at a 10:1 to 100:1 molar ratio of DTPA bicyclic anhydride:protein was radiolabelled with ^{111}In acetate and the EGFR binding properties were evaluated in a direct binding assay using MDA-MB-468 human breast cancer cells as previously reported (7). There was only a slight decrease in the affinity constant (K_a) with increasing DTPA substitution level but no significant decrease in the maximum number of binding sites/cell (B_{max}, Table 1). The K_a for binding of ^{111}In-DTPA-HSA-hEGF to EGFR on MDA-MB-468 cells (2.1-5.1 X 10^7 L/mol) was 15-35 fold lower however than that previously observed for ^{111}In-DTPA-hEGF (K_a ~7.5 X 10^8 L/mol).

Table 1. EGFR Binding Properties of ^{111}In-DTPA-HSA-hEGF Against MDA-MB-468 Human Breast Cancer Cells

Molar Ratio (cDTPAA:HSA-hEGF)	DTPA Substitution (mols DTPA/mol HSA-hEGF)	EGFR Binding Properties * K_a (L/mol X 10^7)	EGFR Binding Properties * B_{max} (Sites/Cell X 10^6)
10:1	1.6 ± 0.6	5.1 ± 1.3	2.0 ± 0.6
25:1	5.6 ± 1.0	4.8 ± 1.3	1.6 ± 0.1
50:1	13.5 ± 2.4	2.1 ± 0.6	1.7 ± 0.1
100:1	22.7 ± 5.0	3.4 ± 0.9	1.4 ± 0.1

* Mean ± SEM of 3-7 experiments.

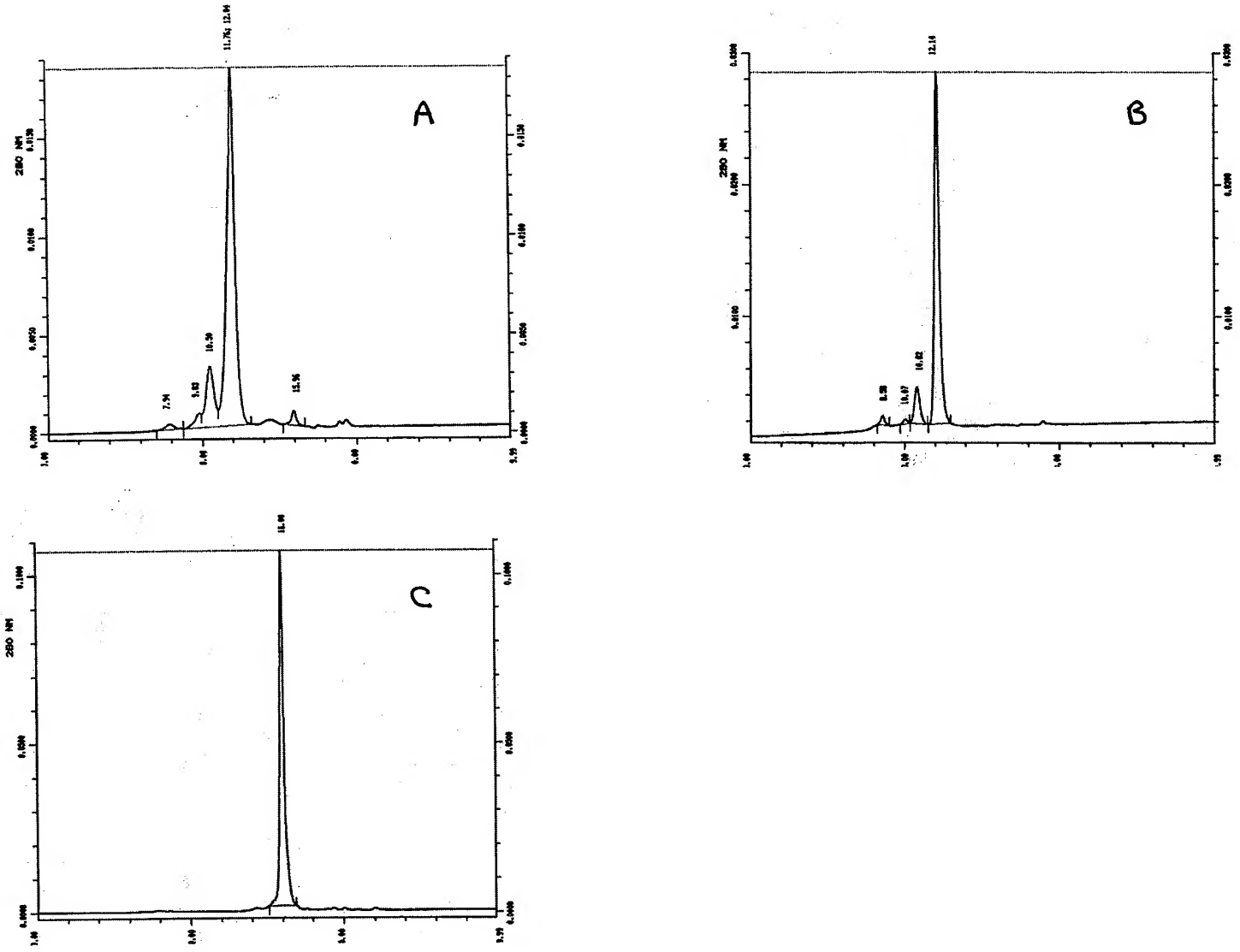

Fig. 3. Size-exclusion HPLC chromatograms of A. HSA-hEGF, B. unconjugated HSA and C. unconjugated hEGF. Samples were analysed on a Progel TSK swxl G2000 column (Supelco, Bellefonte, PA) eluted with 100 mM KH_2PO_4/100 mM Na_2SO_4 pH 7.0 at a flow rate of 1.0 mL/min with detection by UV absorbance at 280 nm.

^{111}In-HSA-hEGF exhibited saturable binding to MDA-MB-468 cells which was decreased more than 20-fold in the presence of an excess (100 nM) of unlabelled hEGF (Fig. 4) indicating that binding to the cells was specific and mediated by EGFR.

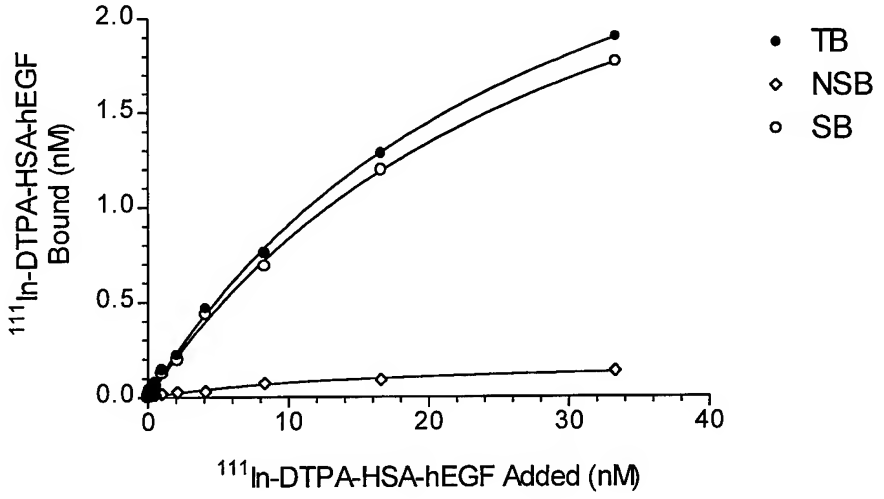

Fig. 4. Representative binding curve for binding of ^{111}In-DTPA-HSA-hEGF to MDA-MB-468 human breast cancer cells. ^{111}In-DTPA-HSA-hEGF was derivatized at 10:1 molar ratio of cDTPAA:protein resulting in substitution of 1-2 DTPA groups per molecule of bioconjugate. TB: Total Binding; NSB: Non-specific binding in the presence of an excess (100 nM) of unlabelled hEGF; SB: Specific Binding (obtained by subtraction of NSB from TB).

These results suggested that conjugation of hEGF with HSA was the main factor responsible for decreasing the binding affinity for the EGFR, but that substitution with multiple DTPA metal chelators on the HSA domain had only a small effect on binding affinity. The data confirmed our original hypothesis that fusion of hEGF with a macromolecule such as HSA could be used to introduce multiple DTPA metal chelators for ^{111}In without adversely effecting binding to the EGFR, although conjugation with HSA reduced the affinity for the receptor.

The internalization and nuclear translocation of the HSA-hEGF bioconjugate in breast cancer cells was evaluated by incubation of fluorescein-derivatized bioconjugate with MDA-MB-468 human breast cancer cells (1-2 X 10^6 EGFR/cell) at 37 °C. Similar to that previously observed for hEGF (4), HSA-hEGF was rapidly internalized into cytoplasmic vesicles in MDA-MB-468 cells within 30 minutes and translocated to form a perinuclear ring of vesicles around the cell nucleus (Fig. 5). The cell nucleus was visualized by counterstaining the cells with the fluorescent nuclear stain, 4'6'-diamidino-2-phenylindole dihydrochloride (DAPI, Boehringer-Mannheim, Laval, PQ).

A B

Fig. 5. A. Visualization of the internalization and nuclear translocation of fluorescein-derivatized HSA-hEGF in MDA-MB-468 human breast cancer cells by fluorescence microscopy. B. Identification of the nucleus in the cells using DAPI.

Cell fractionation experiments were performed by incubating ^{111}In-DTPA-HSA-hEGF with MDA-MB-468 human breast cancer cells at 37 °C for 0.5, 2 or 4 hours and measuring the amount of radioactivity present on the cell surface, internalized into the cytoplasm or imported into the cell nucleus as previously reported for ^{111}In-DTPA-hEGF (4). These studies demonstrated that >70% of ^{111}In-DTPA-HSA-hEGF bound to MDA-MB-468 cells was internalized into the cytoplasm or imported into the nucleus within 0.5 hours at 37 °C (Table 2).

Table 2. Internalization and Nuclear Accumulation of ^{111}In-DTPA-HSA-hEGF in MDA-MB-468 Human Breast Cancer Cells.

Time (hours)	Cell Surface	Cytoplasm	Nucleus
	Percent of Cell-Bound Radioactivity *		
0.5	31.1 ± 0.6	52.6 ± 1.6	16.3 ± 2.6
2.0	34.2 ± 2.6	35.5 ± 2.1	30.3 ± 2.7
4.0	44.5 ± 1.0	33.8 ± 1.2	21.7 ± 2.2

* Mean ± SEM of 6-9 experiments.

The cytoplasmic fraction decreased over a 4-hour period from >50% to approximately 30-35%, but the nuclear fraction increased over the same time period from 16% to 20-30%. The fraction of radioactivity bound to the cell membrane also increased from 30% at 30 minutes to about 45% at 4 hours. The internalization and nuclear translocation of ^{111}In-DTPA-HSA-hEGF bioconjugate in breast cancer cells is important since it is obligatory for the radiotoxic effect of the Auger electrons. These results are therefore very encouraging for the application of ^{111}In-DTPA-HSA-hEGF bioconjugate for targeted Auger electron radiotherapy of EGFR-positive breast cancer.

Task 4: In vitro testing of relative cytotoxicity of ^{111}In-hEGF, chemotherapy and external radiation alone or in combination against EGFR$^+$ human breast cancer cells (months 18-24)

Targeted Auger electron radiotherapy of EGFR-positive human breast cancer using ^{111}In-DTPA-hEGF is a new but investigational anticancer treatment modality. The relative potency of targeted Auger electron radiotherapy for killing breast cancer cells compared to conventional treatments such as chemotherapy or external radiation is not known. It is also not known if there could potentially be advantages in combining targeted Auger electron radiotherapy with conventional treatments.

In order to examine these issues, we conducted experiments to measure the relative cytotoxicity *in vitro* of ^{111}In-DTPA-hEGF, chemotherapy or external radiation against MDA-MB-468 human breast cancer cells. MDA-MB-468 cells were treated *in vitro* with increasing concentrations of ^{111}In-DTPA-hEGF (0-200 pM, 0-34 pCi/cell), doxorubicin (0-200 nM), taxol (0-25 nM), camptothecin (0-100 nM) or with increasing doses of external radiation (0-20 Gy) using a ^{137}Cs source. The growth rate of the cells over a 7-day period was measured by a colorimetric cell viability assay (WST-1, Boehringer-Mannheim) and compared to control, untreated cells. The WST-1 assay measures the activity of the mitochondrial enzyme, succinate-tetrazolium reductase present in living cells to convert the tetrazolium salt, WST-1 (4-[3-[4-iodophenyl]-2-[4-nitrophenyl]-2H-5-tetrazolio]-1,3-benzene disulfonate) to a colored formazan complex. These studies confirmed our previous findings (4) that ^{111}In-DTPA-hEGF was highly radiotoxic to MDA-MB-468 cells. The cells were also slightly growth inhibited by unlabelled hEGF as previously reported (8). The effective dose to reduce the growth of MDA-MB-468 cells by 50% (ED_{50}) was 0.05-0.1 nM for ^{111}In-DTPA-hEGF and >>0.2 nM for unlabelled DTPA-hEGF (Fig. 6 and Table 3).

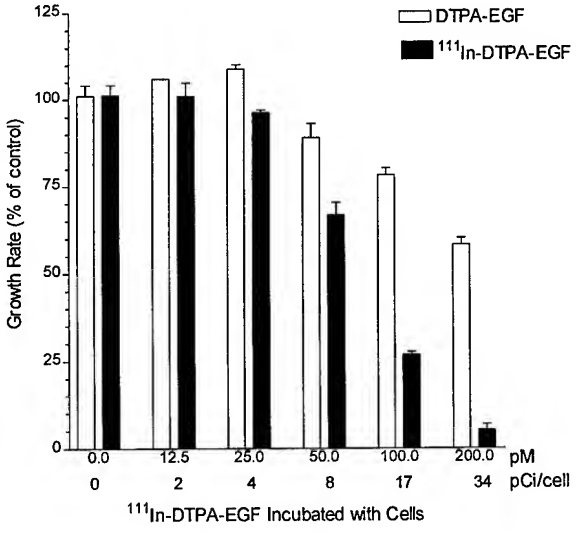

Fig. 6. Effect of treatment of MDA-MB-468 human breast cancer cells with ^{111}In-DTPA-hEGF or unlabelled DTPA-hEGF on the growth rate of the cells over a 7-day period as measured by the WST-1 colorimetric cell viability assay.

The effective dose to reduce the growth of MDA-MB-468 cells by 90% (ED_{10}) was <0.2 nM for ^{111}In-DTPA-hEGF. MDA-MB-468 cells were also growth inhibited by chemotherapeutic agents but the ED_{50} and ED_{10} values were 30-fold to 500-fold higher than those for ^{111}In-DTPA-hEGF (Table 3). Treatment of the MDA-MB-468 cells with 0.05-0.1 nM of ^{111}In-DTPA-hEGF was equivalent to treatment with 2-4 Gy of external radiation. Our results demonstrate that ^{111}In-DTPA-hEGF is a highly effective radiotherapeutic agent for treatment of EGFR-positive breast cancer cells that has a potency (on a molar basis) which is 30-500 times higher than that of commonly used chemotherapeutic drugs.

Table 3. Relative Cytotoxicity of Targeted Auger Electron Radiotherapy using ^{111}In-DTPA-hEGF, Chemotherapy and External Radiation Against EGFR-Positive MDA-MB-468 Breast Cancer Cells.

Treatment	*ED_{50}	†ED_{10}
^{111}In-DTPA-hEGF	0.05-0.1 nM	0.1-0.2 nM
DTPA-hEGF	>0.2 nM	>>0.2 nM
Doxorubicin	12-25 nM	50-100 nM
Taxol	1.5-3 nM	6-12 nM
Camptothecin	12-25 nM	50-100 nM
External Radiation	2-4 Gy	6-10 Gy

*Concentration required to decrease the growth rate of MDA-MB-468 cells by 50%.
†Concentration required to decrease the growth rate of MDA-MB-468 cells by 90%.

Studies are currently in progress to evaluate the cytotoxicity of targeted Auger electron radiotherapy using ^{111}In-DTPA-hEGF in combination with low doses of chemotherapeutic agents and also to evaluate the mechanism of cell death (ie. apoptosis or necrosis). Preliminary data suggest that combining ^{111}In-DTPA-hEGF with low doses of doxorubicin (25-100 nM), captothecin (5-20 nM) or taxol (5-20 nM) can significantly enhance the cytotoxicity against EGFR-positive breast cancer cells.

Task 5: Comparison of the biodistribution and pharmacokinetics of ^{111}In-HSA-hEGF and ^{111}In-hEGF in mice with human breast cancer xenografts (months 20-24)

The tumour and normal tissue accumulation of the novel ^{111}In-DTPA-HSA-hEGF bioconjugate was evaluated and compared with ^{111}In-DTPA-hEGF in athymic mice implanted with subcutaneous (s.c.) MDA-MB-468 human breast cancer xenografts. The breast cancer xenografts were established by s.c. injection of 3-5 X 10^6 MDA-MB-468 cells in growth medium into the hind leg of each animal. After a period of 4-6 weeks, when the tumours had grown to 0.25-0.5 cm in diameter, groups of 3-5 mice were injected i.v. with 1.85 MBq (1-2 μg) of ^{111}In-DTPA-HSA-hEGF or ^{111}In-DTPA-hEGF. The biodistribution of ^{111}In-DTPA-HSA-hEGF was determined at 24, 48 and 72 hours post-injection (Fig. 7).

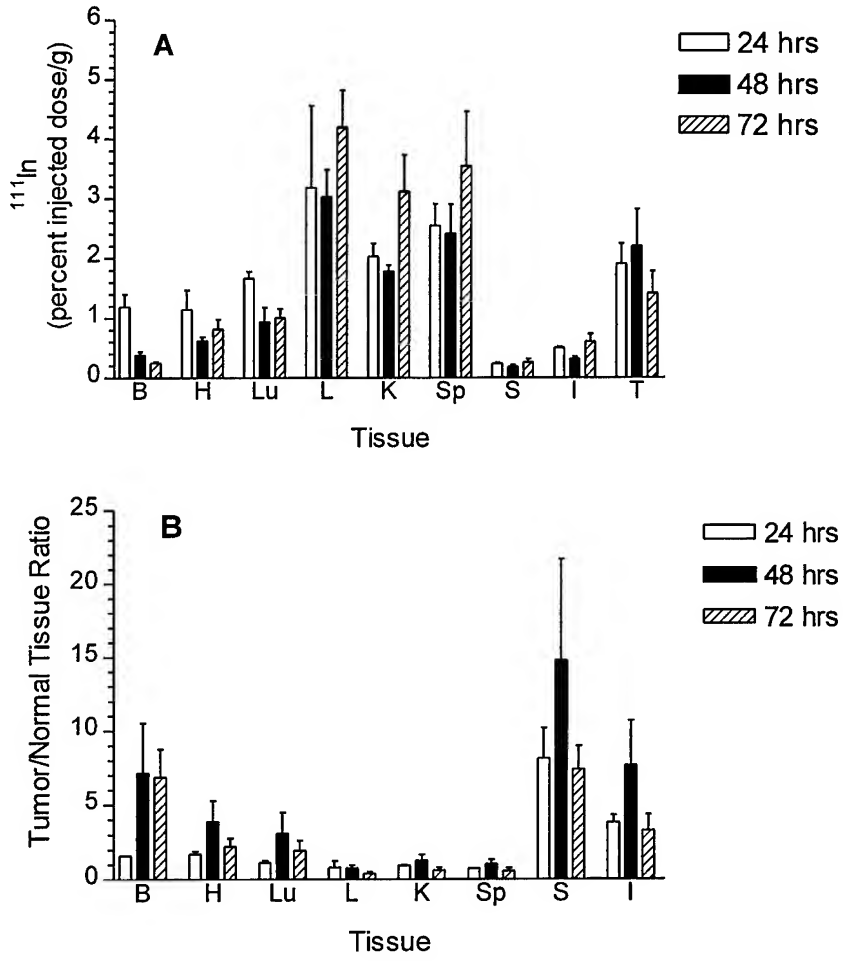

Fig. 7. A. Tumour and normal tissue localization of ^{111}In-DTPA-HSA-hEGF (percent injected dose/g) in athymic mice bearing subcutaneous MDA-MB-468 human breast cancer xenografts at selected times after intravenous injection. B. Tumour/normal tissue ratios.

^{111}In-DTPA-HSA-hEGF rapidly accumulated in MDA-MB-468 human breast cancer xenografts in the mice achieving a tumour concentration of approximately 2-3 percent injected dose/g (% i.d./g) within 24 hours after injection. The concentration of ^{111}In-DTPA-HSA-hEGF in the blood quickly decreased to <0.25% i.d./g within 72 hours after injection. The tumour/blood ratio exceeded 7:1 at 72 hours post-injection indicating tumour localization. Normal tissues which accumulated the greatest amount of ^{111}In-DTPA-HSA-hEGF were the liver, kidneys and spleen.

The biodistribution of ^{111}In-DTPA-HSA-hEGF was compared with that of ^{111}In-DTPA-hEGF at 72 hours post-injection (Table 4). The tumour uptake of ^{111}In-DTPA-HSA-hEGF was not significantly different (t-test, $p<0.05$) from that of ^{111}In-DTPA-hEGF at 72 hours post-injection (1.4 ± 0.4 % i.d./g versus 1.2 ± 0.3 % i.d./g respectively). Normal tissue accumulation of ^{111}In-DTPA-HSA-hEGF in the liver or kidneys was significantly lower however than that of ^{111}In-DTPA-hEGF. Nevertheless, tumour/liver and tumour/kidney ratios for ^{111}In-DTPA-HSA-hEGF and ^{111}In-DTPA-hEGF were both <1:1.

Table 4. Comparison of Tumour and Normal Tissue Localization Properties of ^{111}In-DTPA-HSA-hEGF and ^{111}In-DTPA-hEGF at 72 Hours Post-Injection.

Tissue	Tissue Localization (% i.d./g)		Tumour/Normal Tissue Ratio	
	^{111}In-DTPA-HSA-hEGF*	^{111}In-DTPA-hEGF†	^{111}In-DTPA-HSA-hEGF*	^{111}In-DTPA-hEGF†
Blood	0.25 ± 0.02	0.11 ± 0.02	6.89 ± 1.87	10.34 ± 2.24
Heart	0.82 ± 0.16	0.45 ± 0.10	2.21 ± 0.55	2.70 ± 0.55
Lungs	1.01 ± 0.15	0.52 ± 0.03	1.95 ± 0.67	2.25 ± 0.47
Liver	4.20 ± 0.62	8.56 ± 1.11	0.41 ± 0.11	0.13 ± 0.02
Kidneys	3.12 ± 0.61	19.72 ± 1.63	0.62 ± 0.18	0.06 ± 0.01
Spleen	3.55 ± 0.91	4.45 ± 0.78	0.58 ± 0.17	0.26 ± 0.03
Stomach	0.26 ± 0.06	0.48 ± 0.12	7.42 ± 1.56	2.75 ± 0.81
Intestine	0.60 ± 0.13	0.95 ± 0.10	3.29 ± 1.05	1.23 ± 0.22
Tumour	1.42 ± 0.37	1.17 ± 0.28	na	na

*Mean ± SEM of 7 animals. †Mean ± SEM of 3 animals.

We conclude that conjugation of hEGF with HSA increased the retention of the radiopharmaceutical in the blood more than 2-fold (0.25 % i.d./g versus 0.11 % i.d./g respectively) but unfortunately did not increase the tumour uptake significantly (1.4 % i.d./g versus 1.2 % i.d./g). It is important to appreciate that the HSA-hEGF bioconjugate could nevertheless potentially deliver more ^{111}In radioactivity to the tumour than hEGF due to its higher specific activity as a consequence of substitution of multiple (up to 23) DTPA metal chelators for ^{111}In (see Table 1, p. 9).

Multiple Dose Studies

Another potential strategy that we have explored for increasing the amount of radioactivity to the tumour is to administer multiple doses of ^{111}In-DTPA-hEGF by subcutaneous injection in order to simulate an infusion of the radiopharmaceutical. Preliminary experiments (not shown) demonstrated that there were no significant differences in tumour or normal tissue uptake between intravenous or subcutaneous administration of ^{111}In-DTPA-hEGF. Groups of 4 mice bearing subcutaneous MDA-468 human breast cancer xenografts were injected subcutaneously with a single dose of ^{111}In-DTPA-hEGF (25 μCi, 925 kBq) or with up to five single doses of ^{111}In-DTPA-hEGF and the tumour uptake of radioactivity (kBq/g) was measured at 24 hours after injection of each dose by γ-scintillation counting. The mean tumour uptake of radioactivity (kBq/g) was then plotted versus the tume post-injection (secs) and the cumulative area under the curve (A, kBq.sec/g) calculated by the Trapezoidal Rule (8). These studies demonstrated that the

amount of radioactivity delivered to the tumour as measured by the cumulative area under the curve was increased 10-fold by administering 5 doses of ^{111}In-DTPA-hEGF compared to a single dose (43.0 X 10^6 Bq.sec/g versus 4.3 Bq.sec/g respectively, Table 5). We conclude that administration of multiple doses of the radiopharmaceutical may also be a means of improving tumour uptake of radioactivity to enhance the efficacy of targeted Auger electron radiotherapy of EGFR-positive human breast cancer. This strategy could be applied to ^{111}In-DTPA-hEGF or to ^{111}In-DTPA-HSA-hEGF.

Table 5. Effect of Single Dose versus Multiple Dose Subcutaneous Administration of ^{111}In-DTPA-hEGF on the Cumulative Tumour Uptake of Radioactivity in MDA-MB-468 Human Breast Cancer Xenografts Implanted in Athymic Mice.

Time Interval	Tumour Uptake of Radioactivity (kBq/g)	Cumulative Tumour Uptake of Radioactivity (Bq.sec/g X 10^6)
Single Dose		
0-24 hrs	10.0	0.86
24 hrs-∞	na	3.48
	Total:	4.30
Multiple Dose		
0-24 hrs	10.0	0.86
24-48 hrs	44.0	6.99
48-72 hrs	23.0	11.58
72-96 hrs	19.0	9.07
96-120 hrs	15.0	8.81
120 hrs-∞	na	5.22
	Total:	43.0

Task 6: In vitro testing of the novel ^{111}In-HSA-hEGF bioconjugate for radiotoxicity against MDA-MB-468 and MCF-7 breast cancer cell lines (months 22-26)

The radiotoxicity of ^{111}In-HSA-hEGF against EGFR-overexpressing MDA-MB-468 human breast cancer cells was evaluated by a colorimetric cell growth inhibition assay (WST-1 assay). Approximately 1 X 10^3 cells were seeded in triplicate into wells in a 96-well culture plate then cultured in the presence of 0-1 nM of ^{111}In-DTPA-HSA-hEGF (specific activity 1,135 μCi/μg, 7.5 X 10^7 μCi/μmol) or 0-1 nM of ^{111}In-DTPA-hEGF (specific activity 1,086 μCi/μg, 6.5 X 10^6 μCi/μmol) for 7 days. These studies demonstrated that ^{111}In-DTPA-HSA-hEGF was highly cytotoxic to EGFR-positive human breast cancer cells resulting in a 10-fold decrease in the growth rate at < 1 nM concentration (Fig. 8). The radiotoxicity of ^{111}In-DTPA-HSA-hEGF was

similar to that of ^{111}In-DTPA-hEGF but since the specific activity of ^{111}In-DTPA-HSA-hEGF was about 10-fold higher (7.5 X 10^7 μCi/μmol versus 6.5 X 10^6 μCi/μmol respectively), these results suggest that ^{111}In-DTPA-HSA-hEGF may be 10-fold less potent on a molar basis than ^{111}In-DTPA-hEGF. This could be due to the 15-35 fold lower binding affinity of ^{111}In-DTPA-HSA-hEGF for the EGFR (see Table 1, p. 9). Nevertheless, since the HSA-hEGF bioconjugate can be substituted with as many as 23 DTPA metal chelators for ^{111}In per molecule (see Table 1, p. 9), the lower potency of ^{111}In-DTPA-HSA-hEGF could be easily compensated by its potentially much higher specific activity.

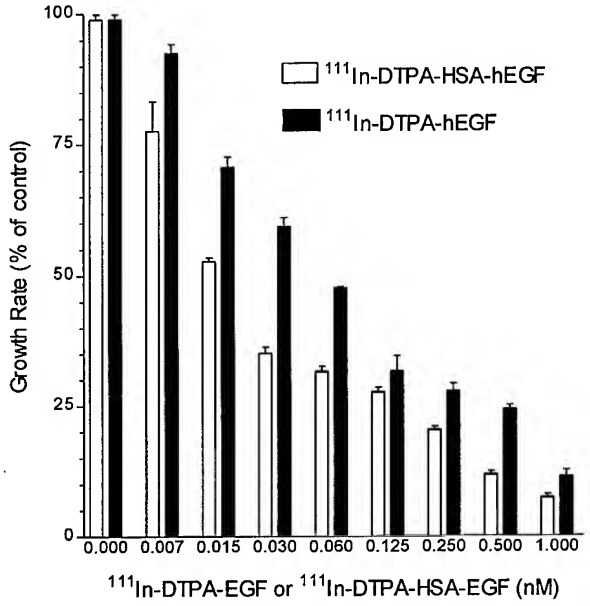

Fig. 8. Comparative cytotoxicity of ^{111}In-DTPA-HSA-hEGF and ^{111}In-DTPA-hEGF against MDA-MB-468 human breast cancer cells. The growth rate of the cells was reduced more than 10-fold by treatment with either radiopharmaceutical.

RESEARCH PLANNED FOR THIRD AND FOURTH YEAR OF PROJECT

A request to extend the termination date for the contract for this project from August 1, 2001 to August 1, 2002 was recently submitted to Ms. Cheryl Miles, Contract Specialist for the US Army BCRP on July 11, 2000. The following therefore represents the planned research for 2000-2001 and also for 2001-2002.

Completion of Current Studies

Task 4: In vitro testing of relative cytotoxicity of ^{111}In-hEGF, chemotherapy and external radiation alone or in combination against subcutaneous EGFR$^+$ human breast cancer cells (months 18-24)

We plan to complete our *in vitro* studies examining the cytotoxicity of ^{111}In-DTPA-hEGF in combination with low doses of chemotherapeutic agents or external radiation. We are also interested in determining the mechanism of cell death (ie. apoptosis or necrosis) and the effect of

targeted Auger electron radiotherapy on cell cycle kinetics. We are especially interested to evaluate DNA damage caused by the Auger electrons using a "Comet" assay which measures DNA strand breaks by an electrophoretic technique. These studies will complete this objective and provide the foundation and rationale for the animal studies described in ***Task 8***.

Task 6: In vitro testing of the novel ^{111}In-HSA-hEGF bioconjugate for radiotoxicity against MDA-MB-468 and MCF-7 breast cancer cell lines (months 22-26)

We plan to conduct more detailed studies to evaluate the cytotoxicity of the novel ^{111}In-DTPA-HSA-hEGF bioconjugate against breast cancer cells. In particular, the selectivity of ^{111}In-DTPA-HSA-hEGF against EGFR-overexpressing breast cancer cells will be evaluated by comparing the relative cytotoxicity against MDA-MB-468 breast cancer cells (1-2 X 10^6 EGFR/cell) and MCF-7 breast cancer cells (1 X 10^4 EGFR/cell). These experiments will be conducted over the next 1-2 months to complete this objective.

New Studies

Task 7: Treatment of nude mice with subcutaneous MDA-MB-468 EGFR$^+$ human breast cancer xenografts with ^{111}In-HSA-hEGF bioconjugate or ^{111}In-hEGF (months 27-39)

A major objective for research over the next year will be to evaluate the efficacy and toxicity *in vivo* of targeted Auger electron radiotherapy using ^{111}In-DTPA-hEGF or ^{111}In-DTPA-HSA-hEGF bioconjugate in athymic mice implanted subcutaneously with MDA-MB-468 human breast cancer xenografts. We are planning to administer multiple doses of the radiopharmaceutical by subcutaneous injection based on our studies (see Table 5, p. 17) which demonstrated a 10-fold improvement in tumour uptake of radioactivity using this strategy. Dose escalation studies will be conducted with multiple administrations of 0.5-2 mCi each of ^{111}In-labelled radiopharmaceutical. Efficacy will be evaluated by tumour growth measurements and toxicity will be evaluated by body weight measurements, peripheral blood cell counts, clinical biochemistry (eg. SCr and ALT) and histopathological examination of the liver and kidneys at necropsy.

Task 8: Treatment of nude mice with MDA-MB-468 human breast cancer xenografts with a combination of ^{111}In-HSA-hEGF (or ^{111}In-hEGF) and chemotherapy (months 40-48)

Our preliminary *in vitro* experiments (see ***Task 4***, p. 12) suggest that combining targeted Auger electron radiotherapy with very low doses of chemotherapeutic agents may be a promising strategy which could significantly enhance the cytotoxicity against breast cancer cells. In the final year of the project, we will therefore conduct studies to examine the anti-tumour efficacy and normal tissue toxicity of ^{111}In-DTPA-hEGF (or ^{111}In-DTPA-HSA-hEGF bioconjugate) combined with low doses of chemotherapeutic agents (eg. doxorubicin or taxol) in athymic mice implanted with subcutaneos MDA-MB-468 human breast cancer xenografts.

KEY RESEARCH ACCOMPLISHMENTS

- A novel human EGF-human serum albumin bioconjugate was constructed which was soluble, pure and mostly monomeric. The human EGF-human serum albumin bioconjugate was derivatized with multiple DTPA metal chelators for ^{111}In while maintaining its receptor binding properties.

- Similar to EGF, the human EGF-human serum albumin bioconjugate was internalized and translocated to the cell nucleus in human breast cancer cells overexpressing the EGFR.

- The human EGF-human serum albumin bioconjugate radiolabelled with ^{111}In was radiotoxic in vitro against human breast cancer cells overexpressing the EGFR.

- The human EGF-human serum albumin bioconjugate radiolabelled with ^{111}In selectively localized in EGFR-positive human breast cancer xenografts implanted in athymic mice achieving tumour/blood ratios >7:1. Tumour uptake was similar to that of ^{111}In-labelled EGF (1-2 percent injected dose/g) but accumulation in the liver and kidneys was much lower.

- Studies comparing the relative cytotoxicity of targeted Auger electron radiotherapy using ^{111}In-labelled human EGF and conventional breast cancer treatments such as chemotherapy or external radiation demonstrated that ^{111}In-labelled human EGF was more than 1000-fold more potent at killing breast cancer cells *in vitro*. In addition, combining very low doses of chemotherapeutic agents with ^{111}In-labelled human EGF may increase the proportion of breast cancer cells killed.

REPORTABLE OUTCOMES

Manuscripts

1. Reilly R.M., Kiarash R., Sandhu J., Lee YW, Cameron R., Hendler A, Vallis K., and Gariépy J. A comparison of epidermal growth factor and monoclonal antibody 528 labelled with indium-111 for imaging human breast cancer. J. Nucl. Med. 41: 903-911, 2000. [Principal author].

2. Reilly RM, Kiarash R, Cameron R, Porlier N, Sandhu, J., Vallis K., Hendler A, Hill, R.P. and Gariépy J. Indium-111 labelled epidermal growth factor is selectively radiotoxic to human breast cancer cells overexpressing the epidermal growth factor receptor. J. Nucl. Med. 41: 429-438, 2000 [Principal author]

3. Wang, J., Chen, P, Su, Z.F. and Reilly, R.M. Initial Evaluation of a Novel EGF-Human Serum Albumin Bioconjugate Labelled with Indium-111 for Targeted Auger Electron Radiotherapy of Breast Cancer. (in preparation) 2000 [Senior responsible author].

4. Chen, P., Mrkobrada, M., Vallis, K. and Reilly, R.M. Comparison of the cytotoxic effects of targeted Auger electron radiotherapy, external γ-radiation and cancer chemotherapeutics

against EGFR-positive human breast cancer cells. (in preparation) 2000. [Senior responsible author].

Abstracts

1. Chen, P., Mrkobrada, M., Vallis, K. and Reilly, R.M. Comparison of the cytotoxic effects of targeted Auger electron radiotherapy, external γ-radiation and cancer chemotherapeutics against EGFR-positive human breast cancer cells. Proc. American Assoc. Cancer Research 91st Annual Meeting P. 706, 2000. [abstract #4490] [Senior responsible author].

2. Reilly, R.M., Chen, P., Mrkobrada, M. and Vallis, K.A. Cytotoxicity of novel targeted Auger electron radiotherapy, external radiation and chemotherapy against EGFR-positive human breast cancer cells. Proc. Department of Defense Era of Hope Breast Cancer Research Program Meeting, Atlanta, GA, June 8-11, 2000. P. 685. [Senior responsible author].

Presentations

1. Reilly, RM. Targeted Auger electron radiotherapy of malignancies. Presented at Nuclear Medicine Rounds, University Hospital, London, ON, April 19, 2000 [Principal author]

Applications for Funding Based on Research

1. Cancer Research Society Inc. Molecular Imaging of the Early Response to Radiotherapy of Breast Cancer. R.M. Reilly (P.I.) and K. Vallis. 2000-2002 $ 49,820 CAN/year (application pending).

2. Breast Cancer Society of Canada. Molecular Imaging of the Early Response to Radiotherapy of Breast Cancer. R.M. Reilly (P.I.) and K. Vallis. 2000-2001 $ 24,930 CAN/year (application pending).

CONCLUSIONS

In conclusion, a novel human serum albumin-human EGF bioconjugate (HSA-hEGF) was constructed which was soluble, bound specifically to EGFR on human breast cancer cells and was internalized and translocated to the cell nucleus. The HSA-hEGF bioconjugate was derivatized with as many as 23 DTPA metal chelators for radiolabelling to high specific activity with the Auger electron-emitting radionuclide, ^{111}In. The ^{111}In-DTPA-HSA-hEGF bioconjugate localized in EGFR-positive MDA-MB-468 human breast cancer xenografts implanted into mice achieving a high tumour/blood ratio (>7:1). The ^{111}In-DTPA-HSA-hEGF bioconjugate was also radiotoxic in vitro to MDA-MB-468 cells. Concurrent studies demonstrated that targeted Auger electron radiotherapy using ^{111}In-DTPA-hEGF is at least 30-500 fold more cytotoxic to EGFR-positive human breast cancer cells than conventional chemotherapeutic agents.

Our results to date are promising for the application of ^{111}In-DTPA-hEGF or ^{111}In-DTPA-HSA-hEGF as potential new radiotherapeutic agents for the treatment of estrogen receptor-negative, hormone-resistant and poor prognosis breast cancer.

REFERENCES

1. Klijn JGM, Berns PMJJ, Schmitz PIM, Foekens JA. The clinical significance of epidermal growth factor receptor (EGF-R) in human breast cancer: a review of 5232 patients. Endocr. Rev. 1992; 13:3-17.

2. Rajkumar T, Gullick WJ. The type I growth factor receptors in human breast cancer. Breast Cancer Res. Treat. 1994; 29: 3-9.

3. Haigler H, Ash JF, Singer SJ, Cohen S. Visualization by fluorescence of the binding and internalization of epidermal growth factor in human carcinoma cells A-431. Proc. Natl. Acad. Sci. USA 1978; 75: 147-160.

4. Reilly RM, Kiarash R, Cameron RG, Porlier N, Sandhu J, Hill RP, Vallis K, Hendler A and Gariepy J. ^{111}In-labeled EGF is selectively radiotoxic to human breast cancer cells overexpressing EGFR. J. Nucl. Med. 2000; 41: 429-438.

5. Adelstein SJ. The Auger process: a therapeutic promise. AJR 1993; 160: 707-713.

6. Reilly RM. Radioimmunotherapy of malignancies. Clin. Pharm. 1991; 10: 359-375.

7. Reilly RM, Kiarash R, Sandhu J, Lee YW, Cameron RG, Hendler A, Vallis K, Gariepy J. A comparison of EGF and MAb 528 labeled with ^{111}In for imaging human breast cancer. J. Nucl. Med. 2000; 41: 903-911.

8. Gibaldi M and Perrier D, eds. Pharmacokinetics 2nd ed. Appendix D. Estimation of Areas. New York: Marcel Dekker Inc. 1982: 445-449.

APPENDICES

^{111}In-Labeled EGF Is Selectively Radiotoxic to Human Breast Cancer Cells Overexpressing EGFR

Raymond M. Reilly, Reza Kiarash, Ross G. Cameron, Nicole Porlier, Jasbir Sandhu, Richard P. Hill, Katherine Vallis, Aaron Hendler, and Jean Gariépy

Division of Nuclear Medicine and Department of Pathology, Toronto General Hospital, University Health Network, Toronto; Department of Radiation Oncology, Princess Margaret Hospital, University Health Network, Toronto; Samuel Lunenfeld Research Institute, Mount Sinai Hospital, Toronto; and Departments of Medical Imaging, Pharmaceutical Sciences, and Medical Biophysics, University of Toronto, Toronto, Ontario, Canada

Our objective was to determine whether the internalization and nuclear translocation of human epidermal growth factor (hEGF) after binding to its cell surface receptor (EGFR) could be exploited to deliver the Auger electron emitter ^{111}In into EGFR-positive breast cancer cells for targeted radiotherapy. **Methods:** hEGF was derivatized with diethylenetriamine pentaacetic acid (DTPA) and radiolabeled with ^{111}In-acetate. The internalization of ^{111}In-DTPA-hEGF by MDA-MB-468 breast cancer cells (1.3×10^6 EGFRs/cell) was determined by displacement of surface-bound radioactivity by an acid wash. The radioactivity in the cell nucleus and chromatin, isolated by differential centrifugation, was measured. The effect on the growth rate of MDA-MB-468 or MCF-7 (1.5×10^4 EGFRs/cell) cells was determined after treatment in vitro with ^{111}In-DTPA-hEGF, unlabeled DTPA-hEGF, or ^{111}In-DTPA. The surviving fraction of MDA-MB-468 or MCF-7 cells treated in vitro with ^{111}In-DTPA-hEGF was determined in a clonogenic assay. The radiotoxicity in vivo against normal hepatocytes or renal tubular cells was evaluated by measuring alanine aminotransferase (ALT) or creatinine levels in mice administered high amounts of ^{111}In-DTPA-hEGF (equivalent to human doses up to 14,208 MBq) and by light and electron microscopy of the tissues. **Results:** Approximately 70% of ^{111}In-DTPA-hEGF was internalized by MDA-MB-468 cells within 15 min at 37°C and up to 15% was translocated to the nucleus within 24 h. Chromatin contained 10% of internalized radioactivity. The growth rate of MDA-MB-468 cells was decreased 3-fold by treatment with ^{111}In-DTPA-hEGF (45–60 mBq/cell). Treatment with unlabeled DTPA-hEGF caused a 1.5-fold decrease in growth rate, whereas treatment with ^{111}In-DTPA had no effect. Targeting of MDA-MB-468 cells with up to 130 mBq/cell of ^{111}In-DTPA-hEGF resulted in a 2-logarithm decrease in their surviving fraction. No decrease in the growth rate or surviving fraction of MCF-7 cells was evident. There was no evidence of hepatotoxicity or renal toxicity in mice administered high amounts of ^{111}In-DTPA-hEGF. Radiation dosimetry estimates suggest that the radiation dose to an MDA-MB-468 cell targeted with ^{111}In-DTPA-hEGF could be as high as 25 Gy with up to 19 Gy delivered to the cell nucleus. **Conclusion:** ^{111}In-DTPA-hEGF is a promising novel radiopharmaceutical for targeted Auger electron radiotherapy of advanced, hormone-resistant breast cancer.

Key Words: breast cancer; epidermal growth factor; ^{111}In; Auger electrons; epidermal growth factor receptor

J Nucl Med 2000; 41:429–438

Over the past decade, numerous studies have investigated the potential for targeted radiotherapy of human malignancies using monoclonal antibodies (MAbs) directed against tumor-associated antigens conjugated with β-particle–emitting radionuclides (radioimmunotherapy) (*1*). Although promising results have been achieved in B-cell lymphomas, radioimmunotherapy has generally been ineffective for the treatment of solid tumors because of dose-limiting bone marrow toxicity. Nonspecific myelotoxicity was associated with high levels of circulating radioactive antibodies perfusing the bone marrow combined with the long pathlength (2–10 mm) of the β particles. Auger electron–emitting radionuclides, such as ^{125}I and ^{111}In, represent an appealing alternative to β-particle emitters for targeted radiotherapy of cancer (*2*). Most Auger electrons have an energy of <30 keV and a very short, subcellular pathlength (2–12 μm) in tissues. Thus, Auger electron emitters can exert their radiotoxic effects on cells only when internalized into the cytoplasm and particularly when they are imported into the cell nucleus (*3*). The high doses of radiation delivered to the cell nucleus from internalized Auger electron–emitting radionuclides are able to cause DNA fragmentation and cell death (*4*). Decay of an Auger electron–emitting radionuclide outside the cell or at the cell surface delivers an insufficient dose of radiation to cause radiotoxicity (*5*). The selective toxicity of Auger electron emitters toward cells that can bind and internalize the radionuclide could, in theory, minimize or even eliminate the nonspecific radiotoxicity against bone marrow stem cells that was previously observed with β emitters in radioimmunotherapy.

^{125}I-iododeoxyuridine (UdR), one of the most widely

Received Jan. 19, 1999; revision accepted Jul. 9, 1999.

For correspondence or reprints contact: Jean Gariépy, PhD, Department of Medical Biophysics, University of Toronto, 610 University Ave., Toronto, Ontario, Canada M5G 2M9.

studied Auger electron–emitting radiopharmaceuticals, is a radiolabeled thymidine analog that is transported into cells and incorporated directly into DNA during S phase (*6*). ^{125}I-UdR is highly radiotoxic to mammalian cells (*7*) but has limitations as a radiotherapeutic agent because of its relative lack of specificity for tumor cells, targeting cells only in S phase, and its extensive deiodination in the liver. Nevertheless, ^{125}I-UdR is currently being investigated for the treatment of bladder cancer (*8*), gliomas (*9*), and hepatic metastases (*10*) in which normal tissue uptake can be minimized by local administration.

The Auger electron emitter ^{111}In is also radiotoxic to cells when internalized (*11*). For example, ^{111}In-oxine, a lipophilic chelate that diffuses nonspecifically into cells used for radiolabeling leukocytes for imaging of infection, can cause DNA damage to lymphocytes (e.g., gaps, breaks, and exchanges in chromosomes) and is potentially radiotoxic and mutagenic to the cells (*12*). ^{111}In-oxine is also radiotoxic to hematopoietic stem cells (*11*), fibroblasts (*5*), and cervical carcinoma cells (*13*). ^{111}In-oxine is not suitable as a radiotherapeutic agent because it internalizes nonspecifically into both normal and malignant cells, but these observations suggest that ^{111}In could be a very effective Auger electron emitter for radiotherapy of cancer if the radionuclide could be specifically targeted and internalized into malignant cells.

One possible strategy for selectively delivering ^{111}In into cancer cells would be to exploit the normal internalization pathway for peptide growth factors after their binding to cell surface receptors. This pathway involves internalization of growth factors and their receptors into cytoplasmic vesicles for proteolytic degradation and, in some cases, may also include nuclear translocation (*14*). Receptors for peptide growth factors are expressed at much higher levels in certain types of malignancies (*15*) than on normal cells and are therefore potential targets for radiopharmaceuticals. For instance, octreotide is an octapeptide analog of somatostatin that has been radiolabeled with ^{111}In (^{111}In-pentetreotide) and used successfully to image tumors that overexpress somatostatin receptors (*16*). The internalization of ^{111}In-pentetreotide and its translocation to the cell nucleus after binding to the somatostatin receptor (*17*) also make the radiopharmaceutical a promising candidate for targeted Auger electron radiotherapy of somatostatin receptor-positive tumors (*18*).

Overexpression of the epidermal growth factor (EGF) receptor (EGFR) at levels up to 100 times higher than that observed on normal epithelial cells has been observed in 30%–60% of human breast cancer biopsies (*19*). EGFR overexpression is an attractive target for the design of novel therapies for breast cancer because it is present in almost all estrogen receptor-negative and hormone-resistant, advanced forms of the disease and is also associated with a poor prognosis (*19*). Such patients are candidates for systemic chemotherapy, but response rates to current regimens are inadequate and long-term survival is poor (*20*). There is an urgent need to develop alternate treatment strategies. Our objective was to investigate the internalization, nuclear translocation, and radiotoxicity of human EGF (hEGF) (Upstate Biotechnology, Lake Placid, NY) radiolabeled with the Auger electron emitter ^{111}In, against EGFR-positive human breast cancer cells, as well as the radiotoxicity of the radiopharmaceutical against normal tissues known to express moderate to high levels of the receptor. Our findings suggest that the application of targeted Auger electron radiotherapy using ^{111}In-hEGF for the treatment of hormone-resistant forms of breast cancer that overexpress the EGFR may be a promising therapeutic strategy.

MATERIALS AND METHODS

Breast Cancer Cells

The human breast cancer cell line MDA-MB-468 was purchased from the American Type Culture Collection (Manassas, VA) and the MCF-7 human breast cancer cell line was obtained from A. Marks (Banting and Best Department of Medical Research, University of Toronto, Toronto, Ontario, Canada). MDA-MB-468 cells were cultured in L-15 medium (Sigma Chemical Co., St. Louis, MO) supplemented with 10% fetal calf serum (FCS), and MCF-7 cells were maintained in Minimal Essential Medium (Sigma) supplemented with 10% FCS, nonessential amino acids, and glutamine (Gibco; Life Technologies, Burlington, ON, Canada).

Radiolabeling of hEGF and Measurement of Receptor Binding In Vitro

hEGF was derivatized with diethylenetriamine pentaacetic acid (DTPA) and radiolabeled with ^{111}In to a specific activity of 3.7–11.1 MBq/μg (22,200–66,600 MBq/μmol) as described (*21*). The radiochemical purity of ^{111}In-DTPA-hEGF as assessed by silica gel instant thin-layer chromatography in 100 mmol/L sodium citrate (pH 5) was 95%–98%. ^{111}In-DTPA-hEGF bound specifically to its receptor on MDA-MB-468 or MCF-7 human breast cancer cells with an affinity constant (K_a) of 7.5×10^8 L/mol or 3.9×10^9 L/mol, respectively. The number of receptors/cell (B_{max}) for ^{111}In-DTPA-hEGF on MDA-MB-468 cells was calculated to be $1.3 \pm 0.7 \times 10^6$, whereas $1.5 \pm 0.7 \times 10^4$ receptors/cell were present on MCF-7 cells.

Fluorescence Microscopy of Breast Cancer Cells

hEGF was derivatized with fluorescein isothiocyanate as described by Haigler et al. (*14*) and purified from excess fluorescein by size-exclusion chromatography on a P-2 minicolumn (BioRad Laboratories, Mississauga, Ontario, Canada) eluted with 150 mmol/L sodium chloride. The intracellular localization of hEGF in MDA-MB-468 human breast cancer cells was evaluated by fluorescence microscopy using fluorescein-hEGF and the fluorescent nuclear stain 4′,6′-diamidino-2-phenylindole dihydrochloride (DAPI; Boehringer-Mannheim, Laval, Quebec, Canada). Briefly, 3×10^4 MDA-MB-468 cells were seeded onto chamber slides (Nunc; Life Technologies) and cultured for 48 h. The adherent cells were washed 3 times with 150 mmol/L sodium chloride, and the slides were incubated in 100 nmol/L fluorescein-hEGF for 1 h at 37°C. The fluorescein-hEGF solution was then removed and the slides were washed 3 times with 150 mmol/L sodium chloride. The slides were then incubated with 100 mmol/L DAPI for 10 min at 37°C and again washed 3 times with 150 mmol/L sodium chloride. The slides were fixed in 0.8% glutaraldehyde (Sigma) and examined with a fluorescence microscope to view the localization of the

DAPI (λ_{excit} 340–380 nm) and fluorescein (λ_{excit} 470–490 nm) probes.

Intracellular Localization of ^{111}In-DTPA-hEGF in Breast Cancer Cells

The intracellular localization of ^{111}In-DTPA-hEGF was determined by incubating the radiopharmaceutical (5 ng) with 3×10^6 MDA-MB-468 cells in 1 mL of 0.1% (weight/volume) human serum albumin in 150 mmol/L sodium chloride in 35-mm culture dishes. Using this amount of ^{111}In-DTPA-hEGF, ~12% of EGFRs were bound by the radiopharmaceutical. The dishes were incubated for 0.25, 0.5, 1, 2, 3, 4, or 24 h at 37°C. The proportion of ^{111}In radioactivity bound to cells at the selected times was determined by transferring cell suspensions to tubes and separating the cell pellet from the supernatant by centrifugation (8600*g* for 5 min). Each fraction was then counted in a γ scintillation counter (Auto Gamma model 5650; Packard Instruments, Downer's Grove, IL). The proportion of ^{111}In radioactivity internalized by cells was determined as described for ^{125}I-EGF by Olsson et al. (*22*) by resuspending and incubating the cell pellet in a 1-mL mixture of 200 mmol/L sodium acetate and 500 mmol/L sodium chloride (pH 2.5) at 4°C for 5 min. The tubes were then centrifuged again to separate the internalized ^{111}In radioactivity (cell pellet) from the noninternalized ^{111}In radioactivity (supernatant).

Nuclear binding of ^{111}In-DTPA-hEGF in MDA-MB-468 human breast cancer cells was determined as described for ^{125}I-EGF (*23*). The MDA-MB-468 cells were first incubated with ^{111}In-DTPA-hEGF, and then the treated cells were transferred to tubes and centrifuged at 600*g* for 10 min to recover the cell pellet. The pellet was then resuspended in a buffer containing 350 mmol/L sucrose, 10 mmol/L KCl, 1.5 mmol/L $MgCl_2$, and 10 mmol/L Tris hydrochloride (pH 7.6) with 0.2% Triton X-100 (BioRad) and 12 mmol/L 2-mercaptoethanol, and the cells were disrupted by sonication for 5 min in an ultrasonic bath. Cell nuclei were isolated by centrifugation of the cell suspension at 900*g* for 10 min. Chromatin was isolated from the nuclei by first washing the nuclear pellet with a buffer containing 200 mmol/L sucrose, 3 mmol/L calcium chloride, and 50 mmol/L Tris hydrochloride (pH 7.6) followed by washing in 140 mmol/L sodium chloride and 10 mmol/L Tris hydrochloride (pH 8.3) and finally by pelleting the suspension at 900*g* for 10 min. The supernatant containing the nucleoplasmic proteins was discarded. The nuclei were then swollen in a small amount of 1 mmol/L Tris hydrochloride (pH 7.9) and centrifuged at 1700*g* for 10 min to separate the chromatin fraction from the supernatant, which contained the nucleoplasm and nuclear membranes.

Growth Inhibition of Human Breast Cancer Cells In Vitro by ^{111}In-DTPA-hEGF

The effect of treating MDA-MB-468 or MCF-7 cells in vitro with ^{111}In-DTPA-hEGF on their growth was determined by incubating 2×10^7 breast cancer cells in 1 mL 150 mmol/L sodium chloride in a sterile 35-mm culture dish in the presence of an excess of ^{111}In-DTPA-hEGF (5 μg, 11.1 MBq) at 37°C for 30 min. The amount of ^{111}In-DTPA-hEGF added represented a 25-fold excess for MDA-MB-468 cells and a 2500-fold excess for MCF-7 cells. The cells were then transferred to a sterile polystyrene culture tube and centrifuged at 600*g* for 5 min. The amount of ^{111}In radioactivity associated with the cell pellet was measured in a radioisotope calibrator (model CRC-12; Capintec, Montvale, NJ) and divided by the number of treated cells to calculate the average amount of ^{111}In radioactivity targeted to each cell (mBq/cell). The cells were then resuspended in growth medium and 5×10^5 cells were seeded into 6 replicate 60-mm culture dishes. The cells were cultured for a period of 7 d. Control dishes contained untreated cells, cells treated with unlabeled DTPA-hEGF (5 μg), or cells incubated with growth medium containing a concentration of ^{111}In-DTPA ([11 kBq/mL] DraxImage; Dorval, PQ, Canada) equivalent to the amount of ^{111}In-DTPA-hEGF bound to the treated cells. On day 1 and day 7, cells were recovered from dishes using a mixture of trypsin and ethylenediaminetetraacetic acid and counted in a hemocytometer. The growth index was defined as the number of cells recovered on day 7 divided by the number of cells recovered on day 1. The average number of cells recovered at the 2 time points and the average growth index were determined and compared for treated and untreated cells. The treated and control dishes each contained cells that were subconfluent throughout the 7-d experiment.

Radiotoxicity of ^{111}In-DTPA-hEGF Against Human Breast Cancer Cells In Vitro

The radiotoxicity of ^{111}In-DTPA-hEGF against MDA-MB-468 or MCF-7 human breast cancer cells was determined in a clonogenic assay. Increasing amounts of ^{111}In-DTPA-hEGF (37 kBq to 2.6 MBq, 0.01–70 μg) were dispensed into sterile 35-mm culture dishes containing 5×10^6 MDA-MB-468 or MCF-7 cells in 1 mL 150 mmol/L sodium chloride. The maximum amounts of ^{111}In-DTPA-hEGF added represented a 1400-fold molar excess for MDA-MB-468 cells and a 140,000-fold molar excess for MCF-7 cells. The dishes were incubated for 30 min at 37°C; then the cells were recovered and assayed for the average amount of ^{111}In radioactivity targeted to each cell (mBq/cell). Sufficient cells (3×10^4–10^6) were then seeded in triplicate into 60-mm sterile culture dishes (Nunclon; Life Technologies) to obtain a measurable number of colonies after culturing for a period of 10 d at 37°C. Control dishes contained cells incubated with growth medium alone. At the end of the culture period, the colonies were stained with methylene blue (1% in a 1:1 mixture of ethanol and water), and the number of colonies (>50 cells/colony) in each dish was counted. The plating efficiency was calculated by dividing the number of colonies observed in each dish by the number of cells seeded. The surviving fraction was calculated by dividing the plating efficiency for the dishes containing treated cells by the plating efficiency for the control dishes.

The survival curves for the treated MDA-MB-468 or MCF-7 breast cancer cells were obtained by plotting the logarithm of the mean surviving fraction for the triplicate dishes versus the amount of ^{111}In radioactivity targeted to the entire cell, internalized into the cytoplasm or associated with the chromatin fraction (mBq/cell). A straight line was then fitted through each of the survival curves by logarithmic linear regression analysis. The D_0 (radiation dose required to reduce the surviving fraction to 0.37) values were estimated from the terminal slope of the regression lines.

Evaluation of Hepatotoxicity and Renal Toxicity of ^{111}In-DTPA-hEGF

To evaluate the potential for acute hepatotoxicity and renal toxicity from ^{111}In-DTPA-hEGF, groups of normal BALB/c mice were injected in the tail vein with 3.7, 9.25, 18.5, or 44 MBq ^{111}In-DTPA-hEGF in 100 μL 150 mmol/L sodium chloride. Control mice received a tail vein injection of 150 mmol/L sodium chloride. Before injection of ^{111}In-DTPA-hEGF and at 24, 48, and 72 h after injection, blood samples were obtained by nicking the tail of each mouse with a sterile scalpel blade and collecting 50-μL samples into heparinized capillary tubes (Microcaps; Fisher Scientific Co., Nepean, Ontario, Canada). The blood samples were

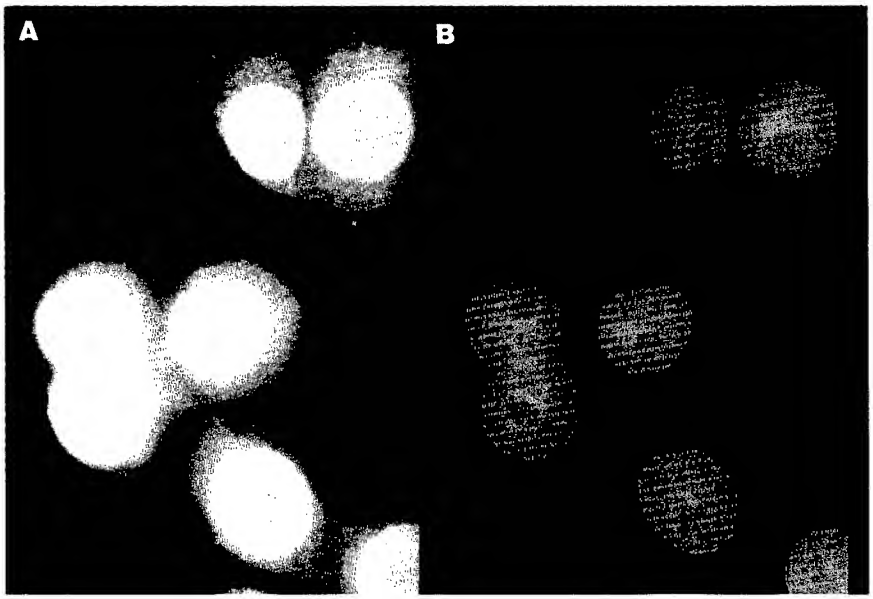

FIGURE 1. Fluorescence microscopy of MDA-MB-468 human breast cancer cells incubated with fluorescein-hEGF for 1 h at 37°C (A) and with nuclear stain DAPI (B). Fluorescein-hEGF was rapidly internalized into cytoplasm of MDA-MB-468 cells and formed a ring surrounding cell nucleus. Cell nucleus was visualized using DAPI.

transferred to microcentrifuge tubes and centrifuged at 10,600*g* for 5 min to separate the plasma. The plasma samples were stored at −10°C for subsequent measurement of alanine aminotransferase (ALT) concentrations by standard clinical biochemistry techniques. At 72 h after injection, the mice were killed by cervical dislocation, and samples of the liver and kidneys were removed, sectioned, and examined by light and electron microscopy for morphologic evidence of hepatic or renal toxicity.

The potential for hepatotoxicity and renal toxicity of ^{111}In-DTPA-hEGF over a longer time period was investigated by administering 2 separate amounts of the radiopharmaceutical to athymic mice (37 and 74 MBq) by tail vein injection separated by an interval of 4 wk. Blood samples were collected before the first administration of the radiopharmaceutical and then every 3–4 d, and the plasma was separated and analyzed for ALT and creatinine concentrations using standard clinical biochemistry techniques. The mice were killed 7 wk after the first administration of the radiopharmaceutical, and the liver and kidneys were removed, sectioned, and examined by light and electron microscopy for morphologic evidence of hepatic or renal toxicity. Animal studies were conducted under an approved Animal Care Protocol (no. 94–036) at the Toronto Hospital and following the Canadian Council on Animal Care guidelines.

RESULTS

Fluorescence Microscopy of Breast Cancer Cells

Fluorescence microscopy of MDA-MB-468 human breast cancer cells incubated with fluorescein-hEGF showed binding to the cell surface, internalization into cytoplasmic vesicles, and localization to the cell nucleus. After 1 h of incubation with fluorescein-hEGF at 37°C, a relatively low level of fluorescence was observed diffusely throughout the cytoplasm of the cells with an intense fluorescence signal associated with the cell nucleus (Fig. 1). The cell nucleus was visualized for comparison using the fluorescent nuclear stain DAPI (Fig. 1).

Intracellular Localization of ^{111}In-DTPA-hEGF in Breast Cancer Cells

^{111}In-DTPA-hEGF was rapidly bound and internalized by MDA-MB-468 cells in vitro at 37°C (Table 1). The internalized fraction increased from ~70% at 15 min of incubation to about 80% at 4 h. After 30 min of incubation of ^{111}In-DTPA-hEGF with cells, a small proportion of ^{111}In radioactivity (~7%) was localized in the cell nucleus and 2.5% was associated with the chromatin fraction (Table 2). The fraction of radioactivity in the cell nucleus increased to >15% at 24 h, with almost 10% associated with the chromatin.

TABLE 1
Kinetics of Binding and Internalization of ^{111}In-DTPA-hEGF in MDA-MB-468 Human Breast Cancer Cells

	Proportion (%)	
Time (h)	^{111}In-DTPA-hEGF bound to MDA-MB-468 cells	Cell-bound ^{111}In-DTPA-hEGF internalized by MDA-MB-468 cells
0.25	41.6 ± 6.8	66.9 ± 2.9
0.5	42.9 ± 7.6	66.2 ± 3.7
1	45.6 ± 8.8	67.4 ± 2.4
2	46.2 ± 9.1	73.1 ± 1.5
3	48.1 ± 10.0	73.0 ± 2.7
4	42.8 ± 8.4	78.3 ± 2.2
24	56.1 ± 7.4	78.6 ± 7.5

Data are expressed as mean ± SEM of 3–6 experiments.

TABLE 2
Kinetics of Nuclear Localization of ^{111}In-DTPA-hEGF in MDA-MB-468 Breast Cancer Cells

Time (h)	Proportion cell-bound ^{111}In-DTPA-hEGF (%)	
	Bound to cell nucleus	Associated with chromatin
0.5	7.2 ± 0.8	2.5 ± 1.4
1	8.2 ± 0.5	2.9 ± 0.9
2	7.1 ± 2.2	3.4 ± 1.1
4	8.2 ± 1.0	3.6 ± 0.6
24	15.5 ± 2.1	9.6 ± 1.3

Data are expressed as mean ± SEM of 3 experiments.

Growth Inhibition of Human Breast Cancer Cells In Vitro by ^{111}In-DTPA-hEGF

Treatment of 2×10^7 MDA-MB-468 or MCF-7 human breast cancer cells in vitro with a 25-fold or 2500-fold molar excess of ^{111}In-DTPA-hEGF (5 μg, 11.1 MBq) resulted in targeting an average of 45–60 mBq ^{111}In-DTPA-hEGF to each cell. However, most ^{111}In-DTPA-hEGF targeted to MCF-7 cells was nonspecifically bound because only a maximum of 3.7 mBq ^{111}In-DTPA-hEGF could, in theory, be specifically targeted to these cells at the receptor saturation conditions used (specific activity of the radiopharmaceutical, 22,200 MBq/μmol; level of expression of the EGFR on these cells, 1.5×10^4 EGFRs/cell). It was assumed that nonspecifically bound ^{111}In-DTPA-hEGF does not undergo receptor-mediated internalization and would not be expected to be radiotoxic.

There was a significant decrease in the growth index of MDA-MB-468 cells treated with ^{111}In-DTPA-hEGF compared with that of untreated cells (1.3 ± 0.2 versus 3.7 ± 0.6, respectively; $P < 0.0001$) (Table 3). MDA-MB-468 cells treated with unlabeled DTPA-hEGF also exhibited a significantly lower growth index compared with that of untreated cells, but the magnitude of the decrease was smaller (2.5 ± 0.6 versus 3.7 ± 0.6, respectively; $P < 0.01$). MDA-MB-468 cells are reported to be growth inhibited by concentrations of EGF > 1 nmol/L (*24*). The concentration of unlabeled DTPA-hEGF in the incubation medium for the growth inhibition assay was 800 nmol/L (i.e., 5 μg/1 mL). The growth index of MDA-MB-468 cells treated with ^{111}In-DTPA, a radiopharmaceutical that does not bind to cells and is not internalized nonspecifically, was not significantly different from the growth index of untreated cells (3.1 ± 0.1 versus 3.7 ± 0.6, respectively; $P = 0.169$). No significant change was found in the growth index of MCF-7 cells, which have a 100-fold lower level of receptors on their surface than do MDA-MB-468 cells (1.5×10^4 versus 1.3×10^6 EGFRs/cell, respectively) treated with ^{111}In-DTPA-hEGF compared with untreated cells (1.7 ± 0.7 versus 2.5 ± 0.5, respectively; $P = 0.193$).

Radiotoxicity of ^{111}In-DTPA-hEGF Against Human Breast Cancer Cells In Vitro

The surviving fraction of MDA-MB-468 human breast cancer cells treated in vitro with ^{111}In-DTPA-hEGF was reduced to <3% when the cells bound 130 mBq/cell ^{111}In-DTPA-hEGF (Fig. 2). The D_0 was approximately 40 mBq/cell for radioactivity targeted to the entire cell but was only 4 mBq/cell when the survival curve was adjusted for radioactivity associated with the chromatin. The D_0 obtained from the survival curve adjusted for radioactivity localized in the cytoplasm was 28 mBq/cell. The amount of ^{111}In radioactivity internalized into the cytoplasm or associated with the chromatin was estimated as 70% and 10%, respectively, of the total ^{111}In radioactivity bound to the cells (Tables 1 and 2). No significant decrease in the surviving fraction of MCF-7 cells was found when up to 133 mBq/cell ^{111}In-DTPA-hEGF was targeted to the cells (Fig. 2). A slight growth-stimulatory effect was observed at low amounts of ^{111}In-DTPA-hEGF bound to MCF-7 cells (<20 mBq/cell).

Evaluation of Hepatotoxicity and Renal Toxicity of ^{111}In-DTPA-hEGF

Graphs shown in Figure 3 depict the concentration of ALT present in the plasma of BALB/c mice as a function of doses of ^{111}In-DTPA-hEGF (3.7–44 MBq) and times after injection. Only at the highest dose of radioactivity administered

TABLE 3
Inhibition of Growth of Human Breast Cancer Cells by Treatment In Vitro with ^{111}In-DTPA-hEGF

Treatment	No. of cells recovered ($\times 10^5$)*					
	MDA-MB-468 cells				MCF-7 cells	
	None	DTPA-hEGF	^{111}In-DTPA	^{111}In-DTPA-hEGF	None	^{111}In-DTPA-hEGF
1 d	2.9 ± 0.2	3.5 ± 0.2	3.3 ± 0.4	4.1 ± 0.2	4.0 ± 0.7	4.2 ± 0.3
7 d	10.6 ± 0.9	8.6 ± 0.3	10.1 ± 0.9	5.2 ± 0.2	6.5 ± 1.0	10.4 ± 0.5
Growth index†	3.7 ± 0.2	2.5 ± 0.2‡	3.1 ± 0.1§	1.3 ± 0.1¶	1.7 ± 0.4	2.5 ± 0.3§

*Mean ± SEM of 3–6 replicates.
†Number of cells recovered at day 7/number of cells recovered at day 1.
‡Significantly different from untreated cells ($P = 0.008$).
§Not significantly different from untreated cells.
¶Significantly different from untreated cells ($P < 0.0001$).

(44 MBq) was there a slight rise in ALT concentration compared with values before administration. No significant changes were observed in ALT or plasma creatinine concentration in comparison with pretreatment values over a 7-wk period in athymic mice administered 2 high amounts of ^{111}In-DTPA-hEGF (37 and 74 MBq) separated by a 4-wk time interval. The plasma ALT concentration in these studies ranged in value from 18 to 46 units/L for treated mice and from 16 to 40 units/L for control mice (normal values in humans, <40 units/L). The plasma creatinine concentration ranged from 60 to 78 μmol/L for treated mice and 60 to 66 μmol/L for control mice (normal values in humans, <105 μmol/L). Morphologic evidence of hepatotoxicity is manifested by subtle mitochondrial changes or proliferation of the smooth endoplasmic reticulum or lysosomes. Renal toxicity is defined by the occurrence of renal tubular degeneration. Such morphologic changes were not observed on the electron micrographs of the liver or kidneys at either early (3 d) or late (7 wk) time points (Fig. 4).

DISCUSSION

This study shows that hEGF radiolabeled with the Auger electron–emitting radionuclide ^{111}In is selectively radiotoxic to human breast cancer cells that overexpress the EGFR. ^{111}In-DTPA-hEGF was rapidly bound by breast cancer cells, internalized into the cytoplasm, and transported to the cell nucleus. We hypothesize that the internalization and nuclear translocation of ^{111}In-DTPA-hEGF delivers the radionuclide in proximity to chromosomal DNA, where emitted Auger electrons are lethal to cells. The radiotoxicity of ^{111}In-DTPA-hEGF in vitro resulted in a significant decrease in the growth rate of MDA-MB-468 human breast cancer cells (1.3×10^6 EGFRs/cell) at relatively low amounts of radioactivity

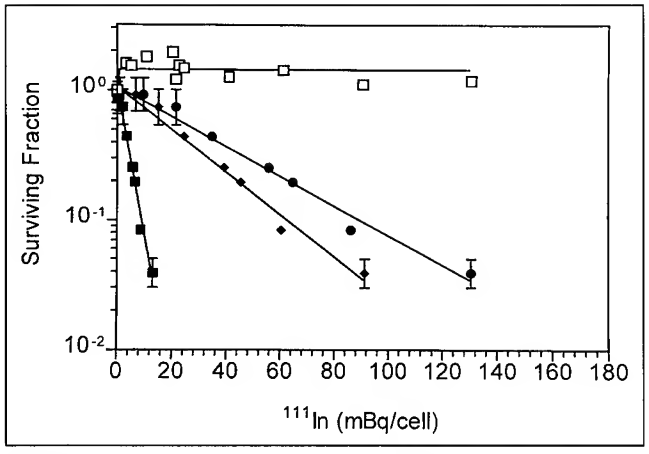

FIGURE 2. Cell survival curves measured in clonogenic assay for MDA-MB-468 (●) or MCF-7 (□) human breast cancer cells treated in vitro with ^{111}In-DTPA-hEGF. Survival curves are also presented for MDA-MB-468 cells treated with ^{111}In-DTPA-hEGF adjusted for proportion of radioactivity localized in cytoplasm (◆) or bound to chromatin (■). Error bars represent SEM of surviving fraction calculated from experiments performed in triplicate dishes.

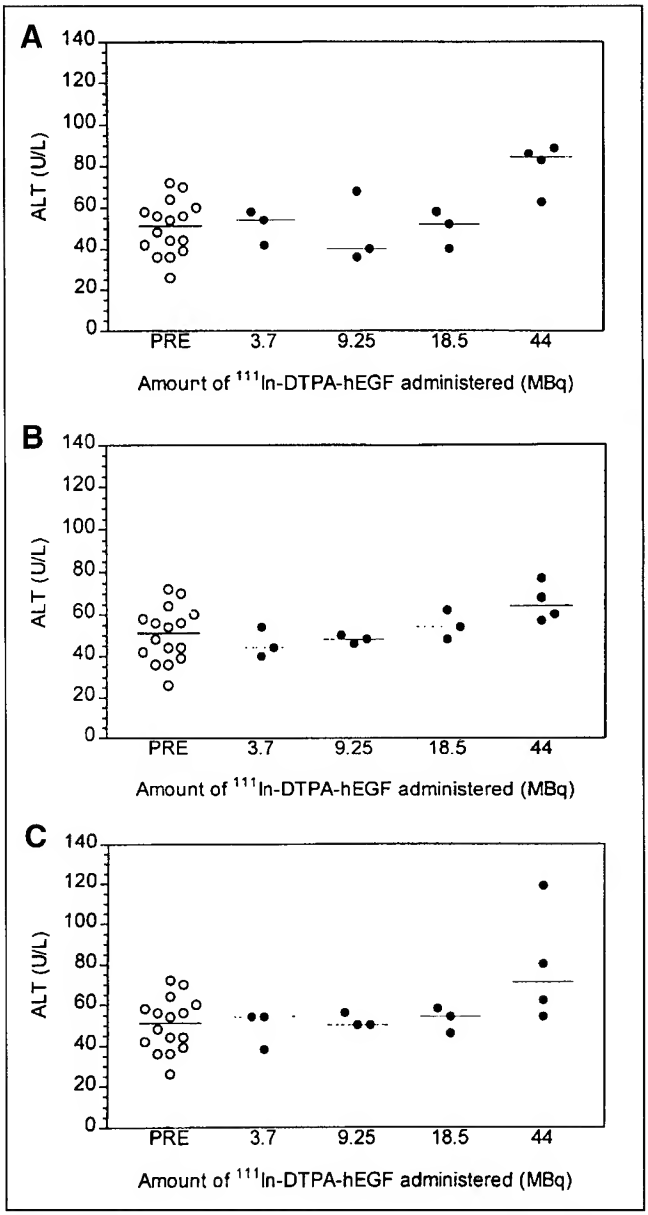

FIGURE 3. ALT concentrations in plasma of BALB/c mice before tail vein injection (PRE) and as function of time after injection (A = 24, B = 48, and C = 72 h) and increasing amounts of injected ^{111}In-DTPA-hEGF (3.7–44 MBq). Only at highest administered amount of radioactivity was there slight rise in ALT concentrations.

targeted to these cells (45–60 mBq/cell). Similarly, a 2-logarithm decrease in the survival of these cells was observed in a clonogenic assay at higher amounts of radioactivity (111–130 mBq/cell). No radiotoxicity was observed against MCF-7 human breast cancer cells that expressed a 100-fold lower level of EGFR (1.5×10^4 receptors/cell), suggesting that the radiopharmaceutical was selectively radiotoxic to cancer cells that overexpress EGFR. In addition, over a 7-wk period, there was no evidence of radiotoxicity to liver or kidneys in mice administered high amounts of ^{111}In-DTPA-hEGF. Liver and kidneys are tissues that express moderate to high levels of EGFR (~10^5 receptors/cell) (*25,26*). These

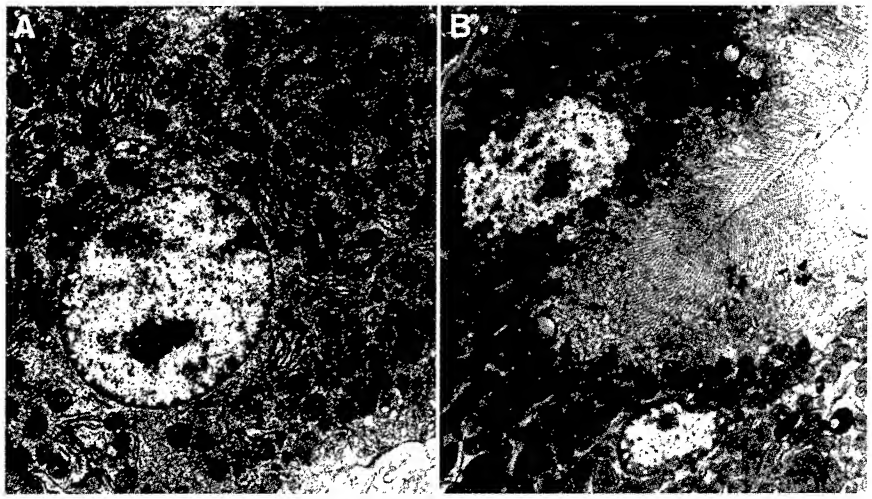

FIGURE 4. Electron micrographs of sections of liver (A) and kidney (B) of athymic mice 7 wk after tail vein injections of 2 separate amounts of ^{111}In-DTPA-hEGF (37 and 74 MBq) separated by 4-wk time interval. No evidence of morphologic damage to liver such as mitochondrial changes, proliferation of smooth endoplasmic reticulum or lysosomes, or steatosis was observed. Similarly, no apparent morphologic damage was apparent to kidneys in form of altered renal tubular structures.

results are thus promising for the application of targeted Auger electron radiotherapy using ^{111}In-DTPA-hEGF for the treatment of EGFR-overexpressing breast cancer in humans.

Fluorescence microscopy revealed that fluorescein-hEGF binds rapidly to MDA-MB-468 cells, is internalized to the cytoplasm, and is subsequently translocated to form a ring of fluorescence surrounding the cell nucleus. The internalization of EGF–EGFR complexes after binding of EGF to its receptor is well documented (*27*), and nuclear localization of EGF has been observed by fluorescence microscopy and other techniques in A431 epidermoid carcinoma cells (*14*), SW948 human colon cancer cells (*23*), fibroblasts (*28*), and hepatocytes (*29*). The proportion of internalized EGF molecules imported to the cell nucleus ranged from 1% to 10% (*30*), but this value increases to 14%–40% under growth-stimulatory conditions (*28,29*) or in the presence of lysosomal protease inhibitors (*31*). It is not known whether EGF remains bound to its receptor during the nuclear translocation process, but the EGFR contains a putative nuclear localization sequence (underlined), RRRHIVRKRTLRR at residues 645–657, that could mediate its nuclear import (*32*). Specific EGFR binding sites on chromatin have also been detected (*30*). The nuclear translocation event of EGF is not currently understood because EGF is thought to affect gene expression indirectly by activation of the ras or phosphatidylinositol intracellular signaling pathways.

^{111}In-DTPA-hEGF was rapidly bound, internalized, and transported to the cell nucleus in MDA-MB-468 breast cancer cells. Interestingly, almost two thirds of the radioactivity in the cell nucleus was associated directly with the chromatin, suggesting that internalized ^{111}In-DTPA-hEGF (perhaps in association with EGFR) may interact directly with nuclear DNA. Similar results have been reported for ^{125}I-EGF by Rakowicz-Szulczynska et al. (*23*) in SW948 human colorectal carcinoma cells that express the EGFR. After incubation of the SW948 cells with ^{125}I-EGF for 24 h at 37°C, >94% of the internalized radioactivity was localized in the cytoplasm and 6% was present in the cell nucleus. Most ^{125}I radioactivity localized in the cell nucleus was associated directly with the chromatin fraction.

Because chromosomal DNA represents a sensitive target in the cell for the radiotoxic effects of Auger electrons emitted by ^{111}In, the cellular distribution of ^{111}In-DTPA-hEGF will control the radiation dose delivered to the nucleus and consequently the radiotoxicity of the radiopharmaceutical. Recently published cellular dosimetry models (*33,34*) of Auger electron–emitting radionuclides deposited in mammalian cells have estimated that the energy deposited in the cell nucleus is 2-fold greater when ^{111}In is localized in the cytoplasm compared with a situation in which the radionuclide is localized on the cell membrane. However, the deposition rate increases by 20- to 35-fold when the radionuclide is localized in the nucleus itself. The radiation doses to an entire cell and to the cell nucleus were calculated (*34*) on the basis of the following distribution pattern of ^{111}In-DTPA-hEGF in MDA-MB-468 breast cancer cells: 20% bound to the cell membrane, 65% internalized into the cytoplasm, and 15% localized in the cell nucleus. It was assumed that the cellular distribution of ^{111}In-DTPA-hEGF under receptor saturation conditions would be similar to that observed (Tables 1 and 2) using conditions under which approximately 12% of the receptors were bound by the radiopharmaceutical. The calculated radiation dose to each MDA-MB-468 cell when targeted to receptor saturation with ^{111}In-DTPA-hEGF (specific activity, 3.7 MBq/μg) was 24.7 Gy, whereas 19.3 Gy was delivered to the cell nucleus (Table 4). More importantly, although only 15% of the ^{111}In-DTPA-hEGF was localized in the cell nucleus, this fraction accounted for 80% of the total radiation dose to the cell nucleus. The ^{111}In-DTPA-hEGF in the cytoplasm was responsible for an additional 18% of the radiation dose to the nucleus, and the remaining 20% fraction of radiopharmaceu-

TABLE 4
Radiation Absorbed Dose Estimates to Cell Nucleus by ^{111}In-DTPA-hEGF Localized in Compartments of MDA-MB-468 Human Breast Cancer Cell*

Cell compartment	$\tilde{A}$† (Bq × s)	S ([Gy/Bq × s] × 10^{-4})	Radiation dose to cell nucleus, $\bar{D}$‡ (Gy)
Membrane	3,357	1.78	0.60
Cytoplasm	10,917	3.18	3.47
Nucleus	2,522	60.30	15.21
		Total	19.28

*Cellular radiation dosimetry model of Goddu et al. (*34*) was used to estimate radiation absorbed dose ($\bar{D}$) to cell nucleus: $\bar{D} = \tilde{A} \times S$, where S is radiation absorbed dose in nucleus (Gy) per unit of cumulated radioactivity in source compartment, $\tilde{A}$ (Bq × s).

†Assumes rapid localization of ^{111}In-DTPA-hEGF in compartment and rate of elimination corresponding to radioactive decay of radionuclide, ^{111}In. $\tilde{A} = A_0/\lambda$, where A_0 is amount of radioactivity localized in compartment at time 0 and λ is radioactive decay constant for ^{111}In (2.83×10^{-6}/s).

‡Based on targeting a single MDA-MB-468 human breast cancer cell with diameter of 10 μm and nucleus with diameter of 6 μm to receptor saturation with ^{111}In-DTPA-hEGF. At concentrations of radioligand leading to receptor saturation, ~48 mBq ^{111}In-DTPA-hEGF would be bound to each MDA-MB-468 cell at specific activity of 3.7 MBq/μg.

tical remaining bound to the cell membrane accounted for only 3% of the radiation dose delivered to the cell nucleus.

The relative radiotoxicity of ^{111}In-DTPA-hEGF toward MDA-MB-468 cells could not be further assigned to distinct intracellular compartments because the radiopharmaceutical is distributed into multiple compartments (i.e., cell membrane, cytoplasm, and nucleus). Nevertheless, by adjusting the survival curves for the proportion of radiopharmaceutical bound to chromatin or present in the cytoplasm, a comparison could be made of the potential differences in radiosensitivity attributed to the radiopharmaceutical being localized in these compartments. The adjusted survival curves (Fig. 2) showed that there could be a 7- to 10-fold greater radiosensitivity of MDA-MB-468 cells when ^{111}In-DTPA-hEGF is bound to the chromatin (D_0, 4 mBq/cell) compared with a situation in which the radiopharmaceutical is localized in the cytoplasm (D_0, 28 mBq/cell) or is distributed evenly in the entire cell (D_0, 40 mBq/cell).

Most normal tissues express very low levels of the EGFR ($<10^4$ receptors/cell) and should not be adversely affected by targeted Auger electron radiotherapy of breast cancer using ^{111}In-DTPA-hEGF. However, the radiopharmaceutical might be radiotoxic to the liver (*25*) and the kidneys (*26*), which exhibit moderate to high levels of the EGFR ($\sim 10^5$ receptors/cell). There was no evidence of radiotoxicity to the liver or kidneys of mice administered high amounts of ^{111}In-DTPA-hEGF corresponding on a MBq/m^2 basis to human amounts of 740–14,208 MBq (surface area of a 25-g mouse is 0.009 m^2 compared with 1.73 m^2 in a 70-kg human). Indeed, over a 7-wk observation period, there were no significant increases in the concentration of ALT or creatinine in the plasma and there were no morphologic lesions in these organs as detected by light or elecron microscopy. The 7-wk observation period should have been sufficient to detect at least early damage to the liver because Wordsworth and Dykes (*35*) showed that increases in serum ALT levels occur within a few days in rats administered high doses of ^{198}Au-colloid (calculated to deliver 30–110 Gy to the liver). Hebard et al. (*36*) found that hepatic injury after administration of ^{198}Au-colloid to rats occurred in 2 phases: an early phase, occurring within the first 2–12 wk, involving fibrosis and infiltration of inflammatory cells into the liver; and a late phase, occurring at 16–40 wk, manifested by severe vasculature damage. Nevertheless, it is possible that very late radiation injury to the liver or kidneys could become evident at time points beyond 7 wk. It is also possible that more subtle forms of liver radiotoxicity may not be seen until the hepatocytes attempt cell division, a process that could require a long period of time for a normally quiescent tissue such as the liver. The radiotoxicity of ^{111}In-DTPA-hEGF against bone marrow stem cells was not measured in this study, but myelotoxicity is not anticipated because <3% of the bone marrow stem cell population has been found to express the EGFR (*37*) and the radiopharmaceutical must specifically bind and internalize in the cells to exert a radiotoxic effect.

One potential limitation to the clinical application of ^{111}In-DTPA-hEGF for targeted radiotherapy of breast cancer is its rapid rate of elimination from the blood, which results in relatively low tumor localization. Studies in athymic mice bearing subcutaneous MDA-MB-468 human breast cancer xenografts administered ^{111}In-DTPA-hEGF showed tumor localization with tumor-to-blood ratios of approximately 12:1, but tumor uptake of the radiopharmaceutical at 72 h after injection was only 2%–3% of injected dose/g (*38*) (Table 5). We believe that the tumor localization of ^{111}In-DTPA-hEGF in vivo can be improved significantly by prolonging its residence time in the blood because the accumulation of ^{111}In-labeled anti-EGFR MAb 528 (which clears much more slowly from the blood than does hEGF) in MDA-MB-468 breast cancer xenografts was 10-fold higher (21% injected dose/g) than that observed for ^{111}In-DTPA-hEGF. We are currently modifying the properties of the hEGF molecule to increase its specific activity and slow its elimination from the blood to improve tumor localization. In future studies, once the pharmacokinetic properties of the radiopharmaceutical have been optimized, we will evaluate the potential for targeted Auger electron radiotherapy of breast cancer in vivo in athymic mice bearing MDA-MB-468 human breast cancer xenografts. Another important issue in the clinical application of ^{111}In-DTPA-hEGF for the treatment of breast cancer is receptor heterogeneity because the radiopharmaceutical is radiotoxic only to cells that express the EGFR and are able to specifically internalize the

TABLE 5
Biodistribution of ^{111}In-DTPA-hEGF at 72 Hours After Injection in Athymic Mice Bearing Subcutaneous MDA-MB-468 Human Breast Cancer Xenografts

	Localization of ^{111}In-DTPA-hEGF	
Tissue	% injected dose/g	Tumor-to-normal tissue ratio
Blood	0.19 ± 0.03	11.85 ± 1.10
Heart	0.57 ± 0.03	3.92 ± 0.50
Lungs	0.89 ± 0.07	2.52 ± 0.28
Liver	9.97 ± 0.07	0.28 ± 0.08
Kidneys	13.69 ± 1.51	0.18 ± 0.04
Spleen	2.29 ± 0.19	0.98 ± 0.11
Stomach	0.54 ± 0.05	4.46 ± 0.97
Intestine	1.77 ± 0.24	1.45 ± 0.38
Tumor	2.24 ± 0.32	NA

NA = not applicable.
Data are expressed as mean ± SEM (n = 5).

radiopharmaceutical. To address this potential problem, it may be necessary to use a cocktail of Auger electron–emitting radiopharmaceuticals. Because EGFR expression is inversely correlated with the expression of estrogen receptors (*19*) or somatostatin receptors (*39*), ^{111}In-DTPA-hEGF could be combined with ^{125}I-estradiol (*40*) or ^{111}In-pentetreotide (*18*) to target a higher proportion of tumor cells in a lesion.

CONCLUSION

We have shown that ^{111}In-DTPA-hEGF was selectively radiotoxic in vitro to human breast cancer cells that overexpress the EGFR. ^{111}In-DTPA-hEGF was rapidly bound by breast cancer cells, internalized into the cytoplasm, and transported to the cell nucleus. We hypothesize that the internalization and nuclear translocation of ^{111}In-DTPA-hEGF delivered the radionuclide in proximity to chromosomal DNA, where the emitted Auger electrons were lethal to the cells. There was no evidence of radiotoxicity associated with the administration of high amounts of the radiopharmaceutical in vivo against normal tissues such as the liver or kidneys, which exhibit moderate to high levels of EGFR expression over a 7-wk observation period in mice. Issues relating to tumor uptake of ^{111}In-DTPA-hEGF in vivo remain to be addressed; nevertheless, these results are encouraging for the application of ^{111}In-DTPA-hEGF in humans for targeted Auger electron radiotherapy of advanced, hormone-resistant breast cancer overexpressing the EGFR.

ACKNOWLEDGMENTS

This research was supported in part by grants from DuPont Pharma, the Susan G. Komen Breast Cancer Foundation (grant 9749), the U.S. Army Breast Cancer Research Program (grant DAMD17–98–1–8171), and the National Cancer Institute of Canada with funds from the Canadian Cancer Society. Parts of this study were presented at the Canadian Association of Nuclear Medicine Meeting, Ottawa, Ontario, Canada (Nov. 10, 1997).

REFERENCES

1. Reilly RM. Radioimmunotherapy of malignancies. *Clin Pharm.* 1991;10:359–375.
2. Adelstein SJ. The Auger process: a therapeutic promise. *AJR.* 1993;160:707–713.
3. Hofer KG, Harris CR, Smith MJ. Radiotoxicity of intracellular Ga-67, I-125 and H-3: nuclear versus cytoplasmic radiation effects in murine L1210 leukemia cells. *Int J Radiat Biol Relat Stud Phys Chem Med.* 1975;28:225–241.
4. Martin RF, Bradley TR, Hodgson GS. Cytotoxicity of an ^{125}I-labeled DNA-binding compound that induces double-stranded DNA breaks. *Cancer Res.* 1979;39:3244–3247.
5. McLean JR, Blakey DH, Douglas GR, Bayley J. The Auger electron dosimetry of indium-111 in mammalian cells in vitro. *Radiat Res.* 1989;119:205–218.
6. Kassis AI, Fayad F, Kinsey BM, Sastry KSR, Taube RA, Adelstein SJ. Radiotoxicity of ^{125}I in mammalian cells. *Radiat Res.* 1987;111:305–318.
7. Chan PC, Lisco E, Lisco H, Adelstein SJ. The radiotoxicity of iodine-125 in mammalian cells. II. A comparative study on cell survival and cytogenetic responses to ^{125}IUdR, ^{131}IUdR, and ^{3}HTdR. *Radiat Res.* 1976;67:332–343.
8. Mariani G, Collechi P, Baldassarri S, et al. Tumor uptake and mitotic activity pattern of 5-[^{125}I]iodo-2′-deoxyuridine after intravesical infusion in patients with bladder cancer. *J Nucl Med.* 1996;37(suppl):16S–18S.
9. Kassis AI, Tumeh SS, Wen PYC, et al. Intratumoral administration of 5-[^{123}]iodo-2′-deoxyuridine in a patient with a brain tumor. *J Nucl Med.* 1996;37(suppl):19S–21S.
10. Macapinlac HA, Kemeny N, Daghighian F, et al. Pilot clinical trial of 5-[^{125}]iodo-2′deoxyuridine in the treatment of colorectal cancer metastatic to the liver. *J Nucl Med.* 1996;37(suppl):25S–29S.
11. Kraal G, Geldorf AA. Radiotoxicity of indium-111. *J Immunol Methods.* 1979;31:193–195.
12. Ten Berge RJM, Natarajan AT, Hardeman MR, et al. Labeling with In-111 has detrimental effects on human lymphocytes: concise communication. *J Nucl Med.* 1983;24:615–620.
13. Danpure HJ, Osman S, Hesslewood IP. Cell damage associated with [^{111}In]oxine labeling of human tumor cell line (HeLa S3). *J Labelled Compd Radiopharm.* 1979;16:116–117.
14. Haigler H, Ash JF, Singer SJ, Cohen S. Visualization by fluorescence of the binding and internalization of epidermal growth factor in human carcinoma cells A-431. *Proc Natl Acad Sci USA.* 1978;75:3317–3321.
15. Mendelsohn J. Growth factor receptors as targets for antitumor therapy with monoclonal antibodies. In: Mendelsohn J, Waldmann H, eds. *Monoclonal Antibody Therapy.* Basel, Switzerland: Karger; 1988:147–160.
16. Krenning EP, Kwekkeboom DJ, Bakker WH, et al. Somatostatin receptor scintigraphy with [^{111}In-DTPA-D-Phe^{1}]- and [^{123}I-Tyr^{3}]-octreotide: the Rotterdam experience with more than 1000 patients. *Eur J Nucl Med.* 1993;20:716–731.
17. Andersson P, Forssell-Aronsson E, Johanson V, et al. Internalization of indium-111 into human neuroendocrine tumor cells after incubation with indium-111-DTPA-D-Phe^{1}-octreotide. *J Nucl Med.* 1996;37:2002–2006.
18. Krenning EP, Valkema R, Kooij PPM, et al. Peptide receptor radionuclide therapy with [indium-111-DTPA-D-Phe]-octreotide [abstract]. *J Nucl Med.* 1997;38(suppl):47P.
19. Klijn JGM, Berns PMJJ, Schmitz PIM, Foekens JA. The clinical significance of epidermal growth factor receptor (EGF-R) in human breast cancer: a review on 5232 patients. *Endocr Rev.* 1992;13:3–17.
20. Fields Jones SM, Burris HA III, Herfindal ET, Gourley DR. Breast cancer. In: Herfindal ET, Gourleey DR, eds. *Textbook of Therapeutics: Drug and Disease Management.* 6th ed. Baltimore, MD: Williams & Wilkins; 1996:1533–1547.
21. Reilly RM, Gariépy J. Factors influencing the sensitivity of tumor imaging using a receptor-binding radiopharmaceutical. *J Nucl Med.* 1998;39:1037–1042.
22. Olsson P, Lindstrom A, Carlsson J. Internalization and excretion of epidermal growth factor-dextran-associated radioactivity in cultured human squamous-carcinoma cells. *Int J Cancer.* 1994;56:529–537.
23. Rakowicz-Szulczynska EM, Rodeck U, Herlyn M, Koprowski H. Chromatin binding of epidermal growth factor, nerve growth factor, and platelet-derived growth factor in cells bearing the appropriate surface receptors. *Proc Natl Acad Sci USA.* 1986;83:3728–3732.
24. Filmus J, Pollak MN, Cailleau R, Buick RN. A human breast cancer cell line with a high number of epidermal growth factor (EGF) receptors has an amplified EGF receptor gene and is growth inhibited by EGF. *Biochem Biophys Res Commun.* 1985;128:898–905.

25. Dunn WA, Hubbard AL. Receptor-mediated endocytosis of epidermal growth factor by hepatocytes in the perfused rat liver: ligand and receptor dynamics. *J Cell Biol.* 1984;98:2148–2159.
26. Fisher DA. Salido EC, Barajas L. Epidermal growth factor and the kidney. *Annu Rev Physiol.* 1989;51:67–80.
27. Osborne CK, Hamilton B, Nover M. Receptor binding and processing of epidermal growth factor by human breast cancer cells. *J Clin Endocrinol Metab.* 1982:55:86–93.
28. Holt SJ, Alexander P, Inman CB, Davies DE. Ligand-induced translocation of epidermal growth factor receptor to the nucleus of NR6/HER fibroblasts is serum dependent. *Exp Cell Res.* 1995;217:554–558.
29. Raper SE, Burwen SJ, Barker ME, Jones AL. Translocation of epidermal growth factor to the hepatocyte nucleus during rat liver regeneration. *Gastroenterology.* 1987;92:1243–1250.
30. Rakowicz-Szulczynska EM, Otwiaska D, Rodeck U, Koprowski H. Epidermal growth factor (EGF) and monoclonal antibody to cell EGF surface receptor bind to the same chromatin receptor. *Arch Biochem Biophys.* 1989;268:456–464.
31. Johnson LK, Vlodavsky I, Baxter JD, Gospodarowicz D. Nuclear accumulation of epidermal growth factor in cultured rat pituitary cells. *Nature.*1980;28:340–343.
32. Laduron PM. Genomic pharmacology: more intracellular sites for drug action. *Biochem Pharmacol.* 1992;44:1233–1242.
33. Faraggi M, Gardin I, de Labriolle-Vaylet C, Moretti J-L, Bok BD. The influence of tracer localization on the electron dose rate delivered to the cell nucleus. *J Nucl Med.* 1994;35:113–119.
34. Goddu SM, Howell RW, Rao DV. Cellular dosimetry: absorbed fractions for monoenergetic electron and alpha particle sources and S-values for radionuclides uniformly distributed in different cell compartments. *J Nucl Med.* 1994;35:303–316.
35. Wordsworth OJ, Dykes PW. A functional and morphological study of liver radiation injury following intravenous injection with colloidal gold (^{198}Au). *Int J Radiat Biol.* 1969;14:497–515.
36. Hebard DW, Jackson KL, Christensen GM. The chronological development of late radiation injury in the liver of the rat. *Radiat Res.* 1980;81:441–454.
37. Waltz TM, Malm C, Nishikawa BK, Wasteson A. Transforming growth factor-alpha (TGF-alpha) in human bone marrow: demonstration of TGF-alpha in erythroblasts and eosinophilic precursor cells and of epidermal growth factor receptors in blastlike cells of myelomonocytic origin. *Blood.* 1995;85:2385–2392.
38. Reilly RM, Kiarash R, Sandhu J, Gariépy J. A comparison of the native peptide ligand and a monoclonal antibody against the epidermal growth factor receptor (EGFR) for imaging human breast cancer [abstract]. *J Nucl Med.* 1998;39:77P.
39. Reubi JC, Waser B, Foekens JA, Klijn JGM, Lamberts SWJ, Laissue J. Somatostatin receptor incidence and distribution in breast cancer using receptor autoradiography: relationship to EGF receptors. *Int J Cancer.* 1990;46:416–420.
40. McLaughlin WH, Milius RA, Pillai KMR, Edasery JP, Blumenthal RD, Bloomer WD. Cytotoxicity of receptor-mediated 16α-[^{125}I]iodo-estradiol in cultured MCF-7 human breast cancer cells. *J Natl Cancer Inst.* 1989;81:437–440.

A Comparison of EGF and MAb 528 Labeled with ^{111}In for Imaging Human Breast Cancer

Raymond M. Reilly, Reza Kiarash, Jasbir Sandhu, Ying Wai Lee, Ross G. Cameron, Aaron Hendler, Katherine Vallis, and Jean Gariépy

Division of Nuclear Medicine and Departments of Pathology and Radiation Oncology, Toronto General Hospital/Princess Margaret Hospital, University Health Network, Toronto; Samuel Lunenfeld Research Institute, Mount Sinai Hospital, Toronto; and Departments of Medical Imaging, Pharmaceutical Sciences, Radiation Oncology, and Medical Biophysics, University of Toronto, Toronto, Canada

Our objective was to compare ^{111}In-labeled human epidermal growth factor (hEGF), a 53-amino acid peptide with anti-epidermal growth factor receptor (EGFR) monoclonal antibody (MAb) 528 (IgG_{2a}) for imaging EGFR-positive breast cancer. **Methods:** hEGF and MAb 528 were derivatized with diethylenetriamine pentaacetic acid (DTPA) and labeled with ^{111}In acetate. Receptor binding assays were conducted in vitro against MDA-MB-468 human breast cancer cells. Biodistribution and tumor imaging studies were conducted after intravenous injection of the radiopharmaceuticals in athymic mice bearing subcutaneous MCF-7, MDA-MB-231, or MDA-MB-468 human breast cancer xenografts or in severe combined immunodeficiency mice implanted with a breast cancer metastasis (JW-97 cells). MCF-7, MDA-MB-231, JW-97, and MDA-MB-468 cells expressed 1.5×10^4, 1.3×10^5, 2.7×10^5, and 1.3×10^6 EGFR/cell, respectively in vitro. **Results:** ^{111}In-DTPA-hEGF and ^{111}In-DTPA-MAb 528 bound with high affinity to MDA-MB-468 cells (K_a of 7.5×10^8 and 1.2×10^8 L/mol, respectively). ^{111}In-DTPA-hEGF was eliminated rapidly from the blood with < 0.2% injected dose/g (%ID/g) circulating at 72 h after injection, whereas ^{111}In-DTPA-MAb 528 was cleared more slowly (3 %ID/g in the blood at 72 h). Maximum localization of ^{111}In-DTPA-hEGF in MDA-MB-468 tumors (2.2 %ID/g) was 10-fold lower than with ^{111}In-DTPA-MAb 528 (21.6 %ID/g). There was high uptake in the liver and kidneys for both radiopharmaceuticals. Tumor-to-blood ratios were greater for ^{111}In-labeled hEGF than for MAb 528 (12:1 versus 6:1), but all other tumor-to-normal tissue ratios were higher for MAb 528. MDA-MB-468 and JW-97 tumors were imaged successfully with both radiopharmaceuticals, but tumors were more easily visualized using ^{111}In-labeled MAb 528. There was no direct quantitative relationship between EGFR expression on breast cancer cell lines in vitro, and tumor uptake of the radiopharmaceuticals in vivo, but control studies showed that tumor uptake was receptor mediated. **Conclusion:** Our results suggest that the tumor uptake in vivo of receptor-binding radiopharmaceuticals is controlled to a greater extent by their elimination rate from the blood than by the level of receptor expression on the cancer cells. Radiolabeled anti-EGFR MAbs would be more effective for tumor imaging in cancer patients than peptide-based radiopharmaceuticals such as hEGF, because they exhibit higher tumor uptake at only moderately lower tumor-to-blood ratios.

Received Apr. 14, 1999; revision accepted Aug. 9, 1999.

For correspondence or reprints contact: Raymond M. Reilly, PhD, Division of Nuclear Medicine, Toronto General Hospital, 585 University Ave., Toronto, Ontario, M5G 2C4 Canada.

Key Words: breast cancer; epidermal growth factor; monoclonal antibody 528; ^{111}In; imaging; epidermal growth factor receptor

J Nucl Med 2000; 41:903–911

The overexpression of cell surface receptors for peptide growth factors is believed to be one process whereby cancer cells acquire the ability to escape normal growth regulatory mechanisms. The presence of the epidermal growth factor receptor (EGFR) at levels up to 100 times higher than on most normal epithelial tissues ($<10^4$ receptors/cell) has been observed in 30%–60% of human breast cancers (*1*). EGFR overexpression in breast cancer is inversely correlated with estrogen receptor (ER) expression and is directly correlated with a lack of response to hormonal therapy with tamoxifen. Several studies have associated this cellular phenotype with poor long-term survival [studies reviewed by Klijn et al. (*1*)].

Patients with disseminated, hormone-resistant breast cancer are candidates for systemic chemotherapy. In addition, new drugs are currently under development that would specifically target the high levels of EGFR expression commonly observed in such malignancies. These drugs include monoclonal antibodies (MAbs) that block the binding of epidermal growth factor (EGF) to the receptor (*2*), tyrosine kinase inhibitors (tyrphostins) that can interfere with the intracellular signaling pathways (*3*), and EGF-conjugated toxins that specifically deliver highly potent inhibitors of protein synthesis into the cytoplasm of the cancer cells (*4*). A logical extension of this strategy, currently being explored in our laboratory (*5*) and by others (*6*), would be to develop novel radiotherapeutic agents that could deliver high doses of radiation specifically to EGFR-positive cancer cells.

The effectiveness of new therapeutic agents targeted to the EGFR will depend on the ability to detect and characterize EGFR-expressing metastatic lesions throughout the body. ER status is commonly measured in biopsies of primary breast cancer lesions at the time of staging to select patients for hormonal therapy. EGFR expression in metastatic disease could be inferred from the inverse correlation

between ER and EGFR expression in breast cancer. This approach may be limited, however, by potential differences in EGFR/ER positivity between the primary tumor and metastases, heterogeneity in receptor expression by the tumor cells, temporal changes in ER/EGFR expression that can occur as a result of treatment (*7*), and the inability to directly evaluate EGFR expression in individual lesions. A survey of the whole body with γ scintigraphy using radiopharmaceuticals specifically targeted to the EGFR would be useful to detect breast cancer lesions and characterize the level of EGFR expression at these sites to appropriately select patients for novel anti-EGFR therapies.

It has been proposed that peptide-based radiopharmaceuticals, such as radiolabeled growth factors, may be more effective for imaging tumors than radiolabeled MAbs (*8*), because of more rapid elimination from the blood and higher tumor-to-blood ratios at early time points. The objective of this study therefore was to directly compare human EGF (hEGF), a 53-amino acid peptide ligand for the EGFR, with antiEGFR MAb 528 (*9*) labeled with ^{111}In for imaging EGFR-positive human breast cancer.

MATERIALS AND METHODS

Breast Cancer Cells

MDA-MB-468 and MDA-MB-231 human breast cancer cells were obtained from the American Type Culture Collection (ATCC, Rockville, MD) and were cultured in L-15 medium (Sigma, St. Louis, MO) supplemented with 10% fetal calf serum (FCS). MCF-7 breast cancer cells were obtained from Dr. A. Marks at the Banting and Best Department of Medical Research, University of Toronto (Toronto, Ontario, Canada) and were cultured in minimal essential medium ([MEM], Sigma) supplemented with 10% FCS, nonessential amino acids, and glutamine (Gibco-BRL, Life Technologies, Burlington, Ontario, Canada). S1 breast cancer cells are a subclone of the MDA-MB-468 breast cancer cell line and express a lower number of EGFR molecules on their surface (*10*). S1 cells were obtained from Dr. R. Buick at the Ontario Cancer Institute (Toronto, Ontario, Canada) and were cultured in L-15 medium supplemented with 10% FCS and 100 nmol/L nEGF. JW-97 human breast cancer cells were obtained by trypsinization of a skeletal metastasis from a patient with advanced disease and then passaged in severe combined immunodeficiency (scid) mice. JW-97 cells were cultured in RPMI 1640 medium (Sigma) supplemented with 10% FCS.

Radiolabeling of EGF

hEGF (Upstate Biotechnology, Lake Placid, NY) was derivatized with diethylenetriamine pentaacetic acid (DTPA) using the bicyclic anhydride of DTPA (Sigma) as previously described (*11*). DTPA-derivatized hEGF showed a single band with an apparent molecular weight (M_r) of 6 kDa by sodium dodecylsulfate polyacrylamide gel electrophoresis (SDS-PAGE) on a tris-Tricine gel (BioRad, Mississauga, Ontario, Canada), indicating no apparent cross-linking of hEGF molecules after reaction with the bicyclic DTPA anhydride. DTPA-conjugated hEGF (25–50 μg) was radiolabeled with ^{111}In-acetate to a specific activity of 3.7–7.4 MBq/μg (22,200–44,400 MBq/μmol). ^{111}In-acetate was prepared by mixing equal volumes of ^{111}In-chloride (>7,400 MBq/mL; MDS-Nordion, Kanata, Ontario, Canada) and 1 mol/L acetate buffer pH 6. ^{111}In-DTPA-hEGF was purified from free ^{111}In by size-exclusion chromatography on a P-2 mini-column (BioRad), then analyzed for radiochemical purity by silica gel instant thin-layer chromatography ([ITLC-SG]; Gelman, Ann Arbor, MI) in 100 mmol/L sodium citrate pH 5. The radiolabeling efficiency was ~80%. The radiochemical purity of ^{111}In-DTPA-hEGF was routinely between 95% and 98%.

hEGF was radioiodinated to a specific activity of 1.5–2.2 MBq/μg (8,880–13,320 mCi/μmol) by incubating 10 μg hEGF with 18.5–37 MBq ^{125}I-sodium iodide (Nycomed-Amersham, Oakville, Ontario, Canada) and 20 μg chloramine-T (Sigma) for 30 s in a glass tube at room temperature. After addition of sodium metabisulfite (40 μg), the radioiodinated hEGF was purified on a P-2 mini-column. The radiolabeling efficiency was ~70%. The radiochemical purity of ^{125}I-hEGF was >95%, as determined by paper chromatography (Whatman, Maidstone, UK) in 85% methanol.

Production and Radiolabeling of MAb 528

HB 8509 hybridoma cells secreting anti-EGFR MAb 528 (IgG_{2a}) were obtained from ATCC and were cultured in RPMI 1640 supplemented with 20% FCS. BALB/c mice were injected intraperitoneally with 1 mL Pristane (2,6,10,14-tetramethylpentadecane; Sigma), followed 3–4 d later with an intraperitoneal injection of 10^7 HB 8509 hybridoma cells in culture medium. After 2 wk, the ascites fluid was removed from the peritoneal cavity, and anti-EGFR MAb 528 was purified from the ascites fluid on a Protein G column (Pierce, Rockford, IL). The purified MAb 528 was desalted on a Sephadex G-25 column (PD-10; Pharmacia, Uppsula, Sweden), concentrated on a Centricon-30 ultrafiltration device (Amicon, Beverly, MA) and diluted to a concentration of 10 mg/mL in 50 mmol/L sodium bicarbonate buffer pH 7.5. The purity of the MAb 528 preparation was assessed by SDS-PAGE under nonreducing conditions on a 4%–20% tris-glycine gel (BioRad). The protein preparation resulted in a single band migrating with an apparent M_r of 150 kDa. Approximately 2 mg MAb 528 were obtained per milliliter of ascites fluid.

MAb 528 (0.5–1 mg), 10 mg/mL in trace-metal free 50 mmol/L sodium bicarbonate buffer pH 7.5 were derivatized with DTPA, using the bicyclic anhydride of DTPA ([cDTPAA]; Sigma) at a molar ratio (cDTPAA:MAb 528) of 10:1 as previously described (*12*). DTPA-MAb 528 was purified by size-exclusion chromatography on a Sephadex G-50 (Pharmacia) mini-column eluted with 50 mmol/L sodium bicarbonate buffer pH 7.5 followed by ultrafiltration through a Centricon-30 device. Analysis of DTPA-MAb 528 by SDS-PAGE under nonreducing conditions on a 4%–20% tris-glycine gel showed a predominant band with an apparent M_r of 150 kDa and a minor band with apparent M_r of 300 kDa, indicating a small proportion (<10%) of MAb 528 molecules cross-linked through cDTPAA. DTPA-MAb 528 (250–500 μg) was radiolabeled to a specific activity of 0.07–0.14 MBq/μg (11,100–22,200 MBq/μmol) with ^{111}In-acetate (37 MBq) and purified from free ^{111}In on a Sephadex G-50 mini-column eluted with 150 mmol/L sodium chloride. The radiolabeling efficiency of DTPA-MAb 528 was ~85%. The radiochemical purity of ^{111}In-DTPA-MAb 528 was routinely >95% determined by ITLC-SG developed in 100 mmol/L sodium citrate pH 5. A nonspecific murine IgG_{2a} (product no. M-9144; Sigma) was derivatized with cDTPAA and radiolabeled with ^{111}In-acetate in an identical manner to MAb 528.

MAb 528 (25–50 μg) was radioiodinated to a specific activity of 0.18–0.37 MBq/μg (27,750–55,500 MBq/μmol) by incubation with 18.5 MBq ^{125}I-sodium iodide in a glass tube precoated with 20 μg

1,3,4,6-tetrachloro-3α,6α-diphenylglycouril (Sigma) at room temperature. Radioiodinated MAb 528 was purified on a Sephadex G-50 mini-column. The radiolabeling efficiency was ~70%. The radiochemical purity of ^{125}I-MAb 528 was >95% as determined by paper chromatography (Whatman No. 1) in 85% methanol.

Measurement of Receptor Binding In Vitro

The binding of radiolabeled hEGF or MAb 528 to its receptor on MDA-MB-468, S1, MDA-MB-231, MCF-7, or JW-97 human breast cancer cells was measured using a direct binding assay. Briefly, aliquots of either radiolabeled hEGF (0.25–80 ng) or MAb 528 (6 ng–4 μg) were dispensed into 35-mm multiwell culture dishes containing 1.5–7 × 10^6 breast cancer cells in 1 mL of 150 mmol/L sodium chloride containing 0.2% weight/volume human serum albumin. After incubation of the dishes at 37°C for 30 min, the cells were transferred to tubes and centrifuged to separate the bound radioactivity (B) in the cell pellet from the free radioactivity (F) in the supernatant. The cell pellet and supernatant were counted in a γ scintillation counter (Packard Auto Gamma 5650; Packard Instruments, Downer's Grove, IL). Nonspecific binding was determined by conducting the assay in the presence of 100 nmol/L hEGF or MAb 528. The affinity constant (K_a) and number of receptors/cell (B_{max}) were determined from a nonlinear fitting of the binding data (*13*).

The receptor-binding fraction (RBF) at infinite receptor excess was determined by incubating 0.5–1 ng ^{111}In-DTPA-hEGF or 10–20 ng ^{111}In-DTPA-MAb 528 with increasing concentrations of MDA-MB-468 breast cancer cells (1–20 × 10^6 cells/mL) for 30 min at 37°C and determining the fraction of radioactivity bound. The RBF at infinite receptor excess was obtained from the intercept on the ordinate (1/RBF) of a plot of total/bound counts versus 1/cell concentration, as previously described by Lindmo et al. (*14*).

Biodistribution and Tumor Imaging Studies

Female, Swiss athymic (nu/nu) mice (4–6 wk old; Charles River Laboratories, Montreal, Quebec, Canada) were injected subcutaneously in the right hind leg with 5 × 10^6–10^7 MDA-MB-468, MDA-MB-231, or MCF-7 human breast cancer cells in growth medium. Mice inoculated with MCF-7 cells also received estradiol supplementation with biweekly subcutaneous injections of 0.5 mg conjugated estrogens (Premarin; Wyeth-Ayerst, St. Laurent, Quebec, Canada), which are required for MCF-7 cells to form tumor xenografts. A freshly obtained biopsy of a skeletal metastasis from a patient with advanced breast cancer (JW-97 cells) was implanted in the left hind leg of scid mice (Samuel Lunenfeld Research Institute). A dose of 1.85–3.7 MBq ^{111}In-DTPA-hEGF (0.5–1 μg) or ^{111}In-DTPA-MAb 528 (25–50 μg) was injected intravenously into mice when the tumors reached a diameter of 0.25–0.5 cm (1–2 cm for JW-97 tumors). One group of control mice received a dose of 1.85–3.7 MBq ^{111}In-DTPA (DraxImage, Dorval, Quebec, Canada). An ^{111}In-labeled nonspecific murine IgG_{2a} was injected into a second group of control mice, whereas ^{111}In-DTPA-hEGF premixed with 500 μg nonradioactive hEGF (ratio of nonradioactive hEGF-to-^{111}In-DTPA-hEGF = 1000:1) was injected intravenously into a third group of control mice.

At 24, 48, and 72 h after injection, groups of mice were killed by cervical dislocation, and the tumor and samples of normal tissues were removed to measure levels of radioactivity. Tissue samples were weighed and counted along with a standard of the injected radiopharmaceutical in a γ counter (Packard Auto Gamma 5650; Packard Instruments) using a window (150–270 keV) to include the 2 γ photopeaks of ^{111}In (172 and 247 keV). The uptake of each radiopharmaceutical by the tumor and normal tissue was expressed as percentage injected dose per gram (%ID/g) of tissue and as tumor-to-normal tissue ratios (T/NT). At 72 h after injection, posterior images of the mice implanted with the MDA-MB-468, JW-97, or MCF-7 human breast cancer xenografts were obtained with a Siemens ZLC-3700 γ camera (Siemens, Knoxville, TN) fitted with a medium-energy, pinhole collimator and interfaced to a General Electric Star 4000i computer (General Electric, Milwaukee, WI). Images were acquired for 10 min using a 20% window centered over the 172 and 247 keV photopeaks of ^{111}In. Animal studies were conducted under an approved Animal Care Protocol (#94-036) at The Toronto Hospital and following the Canadian Council on Animal Care (CCAC) guidelines.

Statistical Analysis

Statistical comparisons were perfomed by ANOVA (F-test, $P < 0.05$) and Student t test ($P < 0.05$).

RESULTS

Binding of Radiolabeled hEGF and MAb 528 to Breast Cancer Cells In Vitro

^{111}In-DTPA-hEGF and ^{111}In-DTPA-MAb 528 bound with high affinity and specificity in vitro to MDA-MB-468 human breast cancer cells (Table 1). K_a was ~6-fold higher for ^{111}In-DTPA-hEGF than for ^{111}In-DTPA-MAb 528. There was no significant difference in binding affinity between ^{111}In- and corresponding ^{125}I-labeled analogs, suggesting that the conjugation of the DTPA chelator to amino groups and their radiolabeling with ^{111}In did not adversely effect the binding of the resulting radiopharmaceutical to the EGFR. The number of binding sites recognized on the MDA-MB-468 cells (B_{max}) was similar for all 4 radiolabeled ligands. There was no significant difference ($P = 0.0847$) in the

TABLE 1
Comparison of Binding of ^{111}In- and ^{125}I-Labeled hEGF or MAb 528 to MDA-MB-468 Human Breast Cancer Cells

Characteristic	^{111}In-DTPA-hEGF	^{125}I-hEGF	^{111}In-DTPA-MAb 528	^{125}I-MAb 528
No. of experiments	6	10	5	4
K_a (L/mol)*	7.5 ± 3.8 × 10^8	7.3 ± 3.6 × 10^8	1.2 ± 0.6 × 10^8	9.4 ± 2.0 × 10^7
B_{max} (sites/cell)†	1.3 ± 0.3 × 10^6	7.2 ± 0.3 × 10^5	9.0 ± 4.5 × 10^5	7.0 ± 3.8 × 10^5

*Affinity constant mean ± SD.
†Maximum number of binding sites/cell (mean ± SD).

fraction of radiolabeled molecules able to bind to EGFRs on MDA-MB-468 cells under conditions of infinite receptor excess for ^{111}In-DTPA-hEGF (0.73 ± 0.17; n = 3) and ^{111}In-DTPA-MAb 528 (0.50 ± 0.04; n = 3).

EGFR expression varied considerably among the 5 breast cancer cell lines tested (Table 2). The highest expression (>10^6 EGFR/cell) was observed on MDA-MB-468 cells, which have an amplified EGFR gene (*10*). MCF-7 and S1 cells exhibited the lowest expression (<10^4 EGFR/cell). MCF-7 is an ER-positive cell line, expected to have low EGFR expression, and the cell line S1 represents a subclone of the MDA-MB-468 cell line, in which the expression of the EGFR gene is downregulated (*10*). JW-97 cells, originally obtained from a biopsy of a skeletal metastasis in a patient with advanced disease, exhibited intermediate levels of EGFR expression, similar to the levels on the MDA-MB-231 breast cancer cell line (1–3 × 10^5 receptors/cell) but almost 30-fold higher than on most normal epithelial tissues (<10^4 EGFR/cell).

Biodistribution and Tumor Imaging Studies

The biodistribution of ^{111}In-DTPA-hEGF and ^{111}In-DTPA-MAb 528 at selected times after an intravenous (tail vein) injection in athymic mice bearing subcutaneous MDA-MB-468 human breast cancer xenografts is shown in Figure 1. The blood levels of ^{111}In-DTPA-hEGF (Fig. 1A) decreased rapidly with <0.8 %ID/g present in the blood at 24 h after injection, decreasing to <0.2 %ID/g at 72 h. Assuming a blood volume of ~2.5 mL for a mouse weighing 25 g, the concentration of ^{111}In-DTPA-hEGF in the blood corresponded to about 1.7%–2.5% of the injected dose of the radiopharmaceutical at 24 h and <0.5% at 72 h. In contrast, the blood levels of ^{111}In-DTPA-MAb 528 (Fig. 1B) decreased more slowly with ~9 %ID/g present in the blood at 24 h after injection, decreasing to 3 %ID/g at 72 h. The concentration of ^{111}In-DTPA-MAb 528 in the blood corresponded to about 21%–25% of the injected dose of the radiopharmaceutical circulating at 24 h after injection, decreasing to about 7%–8% at 72 h.

The normal tissues that accumulated the highest concentrations of the radiopharmaceuticals were the liver and kidneys (Fig. 1). Liver uptake of ^{111}In-DTPA-hEGF (Fig. 1A) was relatively constant, ranging from 8 to 10 %ID/g. The concentration of ^{111}In-DTPA-hEGF in the kidneys increased slightly from about 11 %ID/g at 24 h to 14 %ID/g at 72 h after injection. Approximately 11%–14% of the injected dose of ^{111}In-DTPA-hEGF localized in the liver and 4%–5% in the kidneys, assuming organ weights of 1.4 and 0.36 g, respectively. For ^{111}In-DTPA-MAb 528 (Fig. 1B), liver accumulation ranged from 6 to 8 %ID/g and uptake in the kidneys was 12–17 %ID/g over the time period of 24–72 h after injection. The liver sequestered ~8%–11% of the injected dose of ^{111}In-DTPA-MAb 528, and the kidneys accumulated 4%–6%. There were no significant differences in the concentrations of the 2 radiopharmaceuticals in the liver or kidneys at 72 h.

Maximum localization of ^{111}In-DTPA-hEGF in the MDA-MB-468 human breast cancer xenografts occurred at 72 h after injection (2.2 %ID/g) and was up to 10-fold lower than that observed for ^{111}In-DTPA-MAb 528 (Fig. 1). Maximum tumor uptake of ^{111}In-DTPA-MAb 528 occurred at 24 h after injection (21.6 %ID/g), then decreased to 11–15 %ID/g at 48–72 h after injection. The mean uptake of ^{111}In-DTPA-hEGF in the MDA-MB-468 breast cancer xenografts at 72 h after injection was decreased more than 5-fold by coadministering 500 μg of unlabeled hEGF (0.40 ± 0.15 %ID/g), suggesting that tumor uptake was a receptor-mediated event. Similarly, the uptake of nonspecific ^{111}In-labeled IgG_{2a} into MDA-MB-468 breast cancer xenografts at 72 h after injection (9.13 ± 1.92 %ID/g) was 2-fold lower than that observed for ^{111}In-DTPA-MAb 528, suggesting that uptake of MAb 528 by tumor cells was also receptor mediated. The mean tumor uptake of ^{111}In-DTPA at 72 h after injection was 0.07 ± 0.01 %ID/g.

T/NTs at selected times after administration of the radiopharmaceuticals are shown in Figure 2. Tumor-to-blood ratios increased rapidly for ^{111}In-DTPA-hEGF (Fig. 2A), reaching values of 2.6:1 at 24 h and increasing to 12:1

TABLE 2
Tumor Localization of ^{111}In-DTPA-hEGF and ^{111}In-DTPA-MAb 528 at 72 Hours After Injection as Function of EGFR Expression

Breast cancer xenograft†	EGFR expression‡ (receptors/ cell × 10^5)	Tumor uptake* (%ID/g) ^{111}In-DTPA-hEGF	Tumor uptake* (%ID/g) ^{111}In-DTPA-MAb 528
MCF-7	0.15 ± 0.07	1.95 ± 0.56	8.40 ± 1.60
MDA-MB-231	1.33 ± 0.85	1.46 ± 0.89	18.03 ± 7.87
JW-97	2.71 ± 0.83	0.70 ± 0.07	4.90 ± 1.08
MDA-MB-468	12.80 ± 2.99	2.24 ± 0.32	15.35 ± 2.49

*Mean ± SEM of 3–6 animals per experiment.
†MCF-7, MDA-MB-231, and MDA-MB-468 xenografts were hosted in athymic mice. JW-97 xenografts were hosted in scid mice.
‡EGFR expression determined in vitro with ^{111}In-DTPA-hEGF. Mean ± SD of 3–10 experiments.

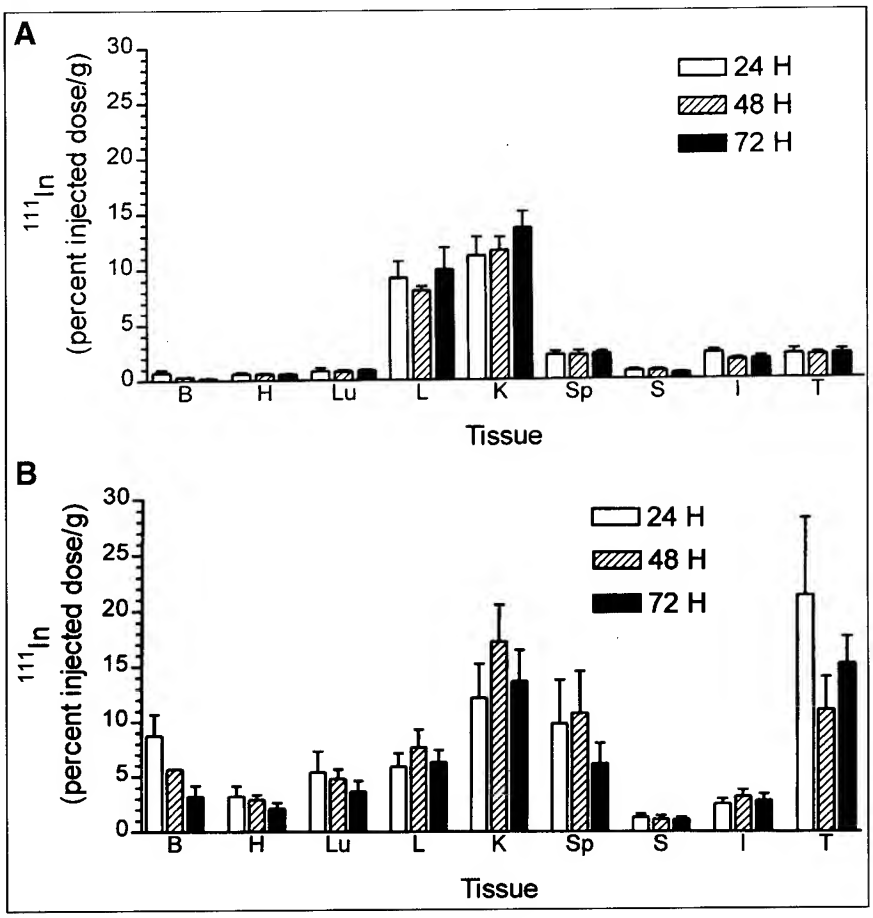

FIGURE 1. Biodistribution at selected times after administration of ^{111}In-DTPA-hEGF (A) and ^{111}In-DTPA-MAb 528 (B) in athymic mice bearing subcutaneous MDA-MB-468 human breast cancer xenografts. Tissues shown are blood (B), heart (H), lungs (Lu), liver (L), kidneys (K), spleen (Sp), stomach (S), intestines (I), and tumor (T).

at 72 h after injection. Tumor-to-blood ratios for ^{111}In-DTPA-MAb 528 (Fig. 2B) increased more slowly, from 2.5:1 at 24 h to about 6:1 at 72 h after injection. T/NTs for ^{111}In-DTPA-hEGF were >2:1 for blood, heart, lungs, stomach, and intestine up to 72 h after injection but were <1:1 for the liver and kidneys as a result of high accumulation of radiopharmaceutical in these normal tissues. Except for the blood, all other T/NTs for ^{111}In-DTPA-MAb 528 were higher than those for ^{111}In-DTPA-hEGF (Fig. 2B). Tumor-to-liver ratios for ^{111}In-DTPA-MAb 528 (1.4:1–3.3:1) were 5- to 11-fold higher than those observed for ^{111}In-DTPA-hEGF, and tumor-to-kidney ratios were 3- to 10-fold greater (0.7:1–1.8:1).

Biodistribution studies in athymic or scid mice bearing subcutaneous MDA-MB-468, MDA-MB-231, JW-97, or MCF-7 human breast cancer xenografts at 72 h after injection of ^{111}In-DTPA-hEGF or ^{111}In-DTPA-MAb 528 showed no direct correlation between the level of tumor uptake of the radiopharmaceuticals and the level of EGFR expression on these cell lines measured in vitro (Table 2). For example, there were no significant differences in the level of accumulation of ^{111}In-DTPA-hEGF (or ^{111}In-DTPA-MAb 528) in MCF-7 or MDA-MB-468 breast cancer xenografts, despite a 100-fold difference in receptor expression ($P = 0.6408$ and $P = 0.0957$, respectively). Similarly, there were no significant differences in the level of accumulation of ^{111}In-DTPA-hEGF (or ^{111}In-DTPA-MAb 528) in MDA-MB-231 and MDA-MB-468 breast cancer xenografts, despite a 10-fold difference in receptor expression ($P = 0.3955$ and $P = 0.6838$, respectively). Nevertheless, the tumor uptake of ^{111}In-DTPA-MAb 528 was 4- to 12-fold higher than that of ^{111}In-DTPA-hEGF in all cases. The localization of either ^{111}In-DTPA-hEGF or ^{111}In-DTPA-MAb 528 was significantly lower in JW-97 tumors than in the MDA-MB-468 breast cancer xenografts ($P = 0.0041$ and $P = 0.0260$, respectively). There was no significant difference in the tumor uptake of ^{111}In-DTPA-hEGF in MDA-MB-231 breast cancer xenografts compared with the JW-97 tumors ($P = 0.427$). Similarly, there was no significant difference in the tumor uptake of ^{111}In-DTPA-MAb 528 between the MDA-MB-231 or JW-97 tumor xenografts ($P = 0.684$).

MDA-MB-468 and JW-97 human breast cancer xenografts expressing 1.3×10^6 or 2.7×10^5 EGFR/cell in vitro, respectively, (Table 1) were successfully imaged with ^{111}In-DTPA-hEGF or ^{111}In-DTPA-MAb 528 at 72 h after injection (Figs. 3 and 4). However, the greater tumor uptake of ^{111}In-DTPA-MAb 528 compared with ^{111}In-DTPA-hEGF resulted in an enhanced definition of the breast cancer xenografts. The liver and kidneys were the major normal

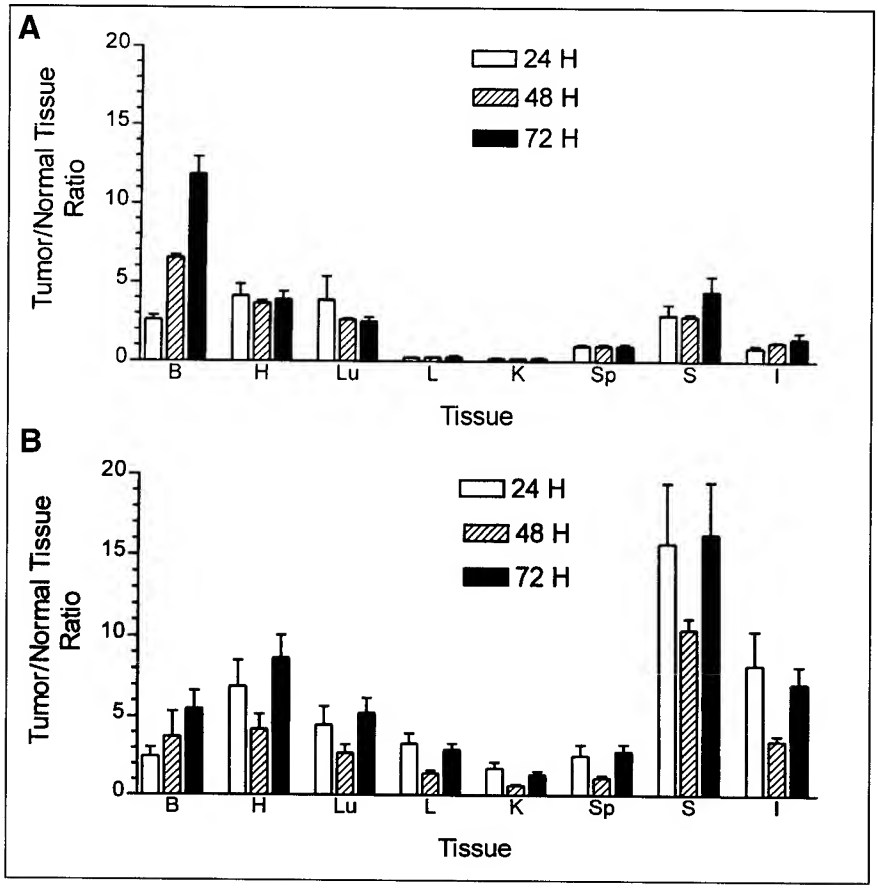

FIGURE 2. T/NTs at selected times after administration of ^{111}In-DTPA-hEGF (A) and ^{111}In-DTPA-MAb 528 (B) in athymic mice bearing subcutaneous MDA-MB-468 human breast cancer xenografts. Tissues shown are blood (B), heart (H), lungs (Lu), liver (L), kidneys (K), spleen (Sp), stomach (S), and intestines (I).

organs visualized on the images, but there was also some uptake in the area of the submaxillary glands. The levels of circulating radioactivity and whole-body radioactivity were considerably lower on the images obtained using ^{111}In-DTPA-hEGF than on those obtained with ^{111}In-DTPA-MAb 528. MCF-7 xenografts could not be visualized with either ^{111}In-DTPA-hEGF or ^{111}In-DTPA-MAb 528 because of their small size (<0.2 cm in diameter).

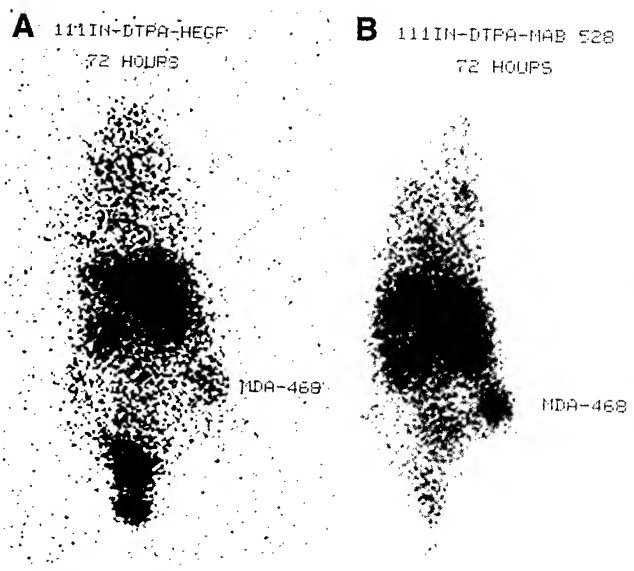

FIGURE 3. Posterior whole-body images of athymic mouse bearing subcutaneous MDA-MB-468 human breast cancer xenograft at 72 h after injection of ^{111}In-DTPA-hEGF (A) or ^{111}In-DTPA-MAb 528 (B). Tumor is visualized with either radiopharmaceutical but is more clearly defined with ^{111}In-DTPA-MAb 528.

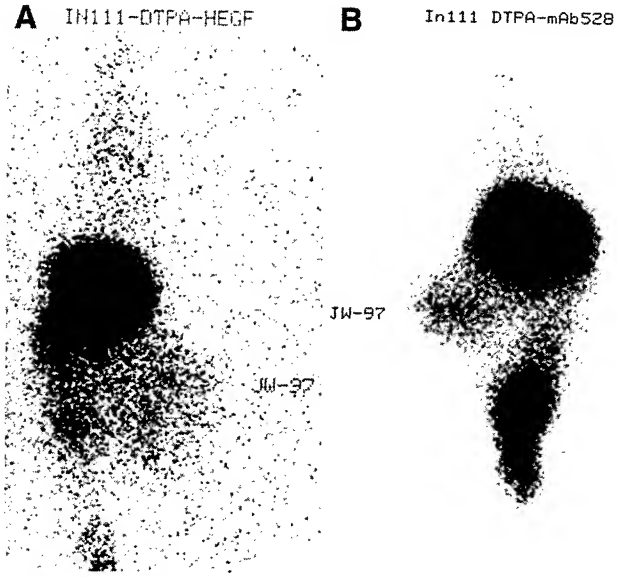

FIGURE 4. Posterior whole-body images of scid mouse bearing subcutaneous JW-97 human breast cancer xenograft at 72 h after injection of ^{111}In-DTPA-hEGF (A) or ^{111}In-DTPA-MAb 528 (B). Tumor is visualized with either radiopharmaceutical but is more clearly defined with ^{111}In-DTPA-MAb 528.

DISCUSSION

Our objective was to compare a peptide-based radiopharmaceutical and a MAb directed against the same cell-surface receptor for imaging of human breast cancer. A systematic evaluation of the localization profiles of these 2 different radiopharmaceuticals was conducted in breast cancer xenografts expressing a broad range of EGFR levels. EGFR-positive breast cancer xenografts hosted in immunocompromised mice were successfully imaged using hEGF, a 53-amino acid peptide ligand (M_r, 6 kDa) for the receptor or anti-EGFR MAb 528 (M_r, 150 kDa) labeled with ^{111}In. The tumor uptake observed with ^{111}In-DTPA-MAb 528 was 7- to 10-fold higher than that observed for ^{111}In-DTPA-hEGF. As a result, the images of the breast cancer xenografts were much clearer with ^{111}In-DTPA-MAb 528, indicating that in certain situations MAbs are more effective tumor-targeting vehicles than are peptide growth factors for receptor imaging of cancer. The higher tumor uptake observed with ^{111}In-DTPA-MAb 528 was likely the result of its slower elimination from the blood, which permitted a greater proportion of the injected dose of the radiopharmaceutical to diffuse into the extravascular space and bind to receptors on breast cancer cells. The higher accumulation of radioactivity in the MDA-MB-468 breast cancer xenografts observed for ^{111}In-DTPA-MAb 528 was not the result of a higher receptor binding affinity, because cell-binding assays showed that the affinity constant for ^{111}In-DTPA-MAb 528 was actually 6-fold lower than that for ^{111}In-DTPA-hEGF ($K_a = 1.2 \times 10^8$ versus 7.5×10^8 L/mol, respectively; Table 1).

^{111}In-DTPA-hEGF was rapidly eliminated from the blood in the animals with <2%–3% of the injected dose remaining in the circulation at 24 h after injection and <1% at 72 h. Two possible mechanisms could explain the rapid blood clearance of ^{111}In-DTPA-hEGF: (a) sequestration by normal tissues that have high levels of EGFR expression (e.g., liver and kidneys), and (b) a high proportion of renal elimination. ^{111}In-DTPA-MAb 528 was eliminated much more slowly from the blood than ^{111}In-DTPA-hEGF, with 25%–30% of the injected dose present in the circulation at 24 h after injection and 10% at 72 h. The slow elimination of ^{111}In-DTPA-MAb 528 from the blood was the result of its large molecular size (M_r, 150 kDa), which prevented its filtration at the glomerulus, a process restricted to proteins with $M_r < 60$ kDa.

Normal hepatocytes exhibit moderate-to-high levels of EGFR expression (8×10^4–3×10^5 EGFR/cell) (*15,16*), and specific receptors for ^{125}I-EGF have been detected in vitro in rat kidney homogenates (*17*) and on renal tubular cells (*18*). The liver has also been shown to have a high capacity to extract ^{125}I-EGF from the circulation (*16,19*). ^{125}I-EGF taken up by hepatocytes is primarily internalized into lysosomes and degraded, but a fraction of internalized EGF molecules are transported by a nonlysosomal pathway and secreted into the bile (*19*). In this study, the liver and kidneys accumulated the highest concentrations of ^{111}In-DTPA-hEGF and ^{111}In-DTPA-MAb 528. Although ^{125}I-labeled EGF has also been reported to exhibit high liver and kidney uptake, radioactivity was cleared from these organs within a few hours (*20–22*). For example, in rats administered ^{125}I-labeled hEGF, >90% of liver radioactivity was cleared within 90 min (*19*). In contrast, the concentration of ^{111}In radioactivity in the liver and kidneys of mice administered ^{111}In-DTPA-hEGF or ^{111}In-DTPA-MAb 528 remained relatively constant up to 72 h after injection (Fig. 1). The clearance of radioactivity from the liver and kidneys after administration of ^{125}I-labeled hEGF is thought to be the result of binding of the radioligand to cell surface receptors on hepatocytes or renal tubular cells, followed by internalization and degradation to free ^{125}I and ^{125}I-iodotyrosine. These catabolites are then exported from the cells and eliminated (*23*). ^{111}In-DTPA-hEGF may follow a similar biologic pathway involving its binding and internalization by hepatocytes or renal tubular cells and degradation by intracellular proteases. However, in the case of ^{111}In-DTPA-hEGF, the final catabolites are likely ^{111}In-DTPA covalently linked to 1 of the 2 lysine residues (K_{28} or K_{48}) or to the N-terminal asparagine. These terminal catabolites would not be recognized by amino acid transporters and therefore would be retained within the cells (*24*). ^{111}In-DTPA-MAb 528 may undergo catabolic fate similar to that of ^{111}In-DTPA-hEGF through its specific binding to cell surface receptors followed by internalization and degradation to catabolites that are retained by cells. Binding of ^{111}In-DTPA-MAb 528 to hepatocytes could be mediated by binding to EGFRs and also to Fc receptors (*25*).

Because hEGF is a peptide, it is readily filtered at the glomerulus and excreted into the urine. ^{125}I-labeled EGF is cleared from the blood by glomerular filtration and is secreted by the proximal renal tubules after binding to receptors on renal tubular cells (*26–28*). ^{125}I-labeled EGF is not reabsorbed by the renal tubules (*28*). It is likely that ^{111}In-labeled hEGF is excreted by a similar mechanism. Renal excretion was the major factor that resulted in the rapid decrease in the blood concentration of ^{111}In-DTPA-hEGF, because sequestration by the liver and kidneys accounted for only 11%–14% and 4%–5% of the injected dose of the radiopharmaceutical, respectively.

Although there was a relatively high accumulation of the radiopharmaceuticals by normal tissues such as the liver and kidneys, both ^{111}In-DTPA-hEGF and ^{111}In-DTPA-MAb 528 localized sufficiently in the MDA-MB-468 and JW-97 human breast cancer xenografts to visualize the tumor by γ scintigraphy at 72 h after injection (Figs. 3 and 4). The images obtained with ^{111}In-DTPA-hEGF and ^{111}In-DTPA-MAb 528 also showed relatively high normal tissue uptake by the liver and kidneys for the reasons discussed, as well as localization of radioactivity in the area of the submaxillary glands. The normal liver and kidney accumulation of both radiopharmaceuticals could limit their clinical usefulness for the detection of liver or adrenal gland metastases in breast cancer patients. The submaxillary glands are responsible for EGF synthesis (*29*), and it is possible that receptors may be present in these tissues to bind and store the newly synthe-

sized growth factor. EGF conjugated with other radionuclides has also been shown to localize in EGFR-positive tumors. Capala et al. (*30*) showed that ^{99m}Tc-EGF was selectively retained in the brains of rats inoculated with glioma cells transfected with the EGFR gene but not in normal rats. Rusckowski et al. (*31*) imaged A431 squamous cell carcinoma xenografts (2×10^6 EGFR/cell) hosted in athymic mice, with ^{99m}Tc-EGF achieving tumor-to-blood ratios of 4:1 at 12 h after injection. Cuartero-Plaza et al. (*32*) detected squamous cell lung carcinoma in 6 of 9 cancer patients by γ scintigraphy using ^{131}I-EGF. To our knowledge, however, this is the first report of successful imaging of EGFR-positive human breast cancer using ^{111}In-labeled EGF or anti-EGFR MAb 528.

The level of accumulation of ^{111}In-DTPA-MAb 528 (11–22 %ID/g; Fig. 1B) in the MDA-MB-468 and JW-97 tumors was 7- to 10-fold higher than that observed for ^{111}In-DTPA-hEGF, allowing much clearer definition of the tumor despite the slightly lower tumor-to-blood ratios associated with ^{111}In-DTPA-MAb 528 (5:1 versus 12:1; Fig. 2). Goldenberg et al. (*33*) successfully imaged MDA-MB-468 human breast cancer xenografts using the anti-EGFR MAb 225 (IgG_{2a}) labeled with ^{111}In, but the tumor uptake was more than 5-fold lower than we observed with ^{111}In-labeled MAb 528 (4 versus 22% ID/g). Because ^{111}In labeled MAb 225 has already been shown to successfully image squamous cell lung carcinoma in patients (*34*), the higher tumor uptake observed with ^{111}In-DTPA-MAb 528 in the MDA-MB-468 human breast cancer xenograft model in this study, is encouraging for the ultimate clinical application of this new radiopharmaceutical for the diagnostic imaging of EGFR-positive breast cancer in humans.

It is interesting to speculate on the reasons why we observed no direct quantitative relationship between the level of receptors measured on the breast cancer cell lines in vitro and the level of accumulation of either radiopharmaceutical in the corresponding breast cancer xenografts in vivo. This finding was not the result of the inactivation of either hEGF or MAb 528 on radiolabeling with ^{111}In, because cell binding assays showed that both radiopharmaceuticals exhibited their expected receptor binding properties (Table 1). Furthermore, biodistribution studies in animals bearing MDA-MB-468 breast cancer xenografts administered a nonspecific ^{111}In-labeled IgG_{2a} or ^{111}In-DTPA-hEGF mixed with an excess of nonradioactive hEGF (to compete with radiolabeled-hEGF for receptor binding) showed a 2- to 5-fold decrease in tumor uptake, suggesting that the tumor accumulation of the radiopharmaceuticals was receptor mediated.

One possible explanation for our inability to observe a direct correlation between receptor expression levels in vitro and tumor uptake of the radiopharmaceuticals in vivo is that in the context of tumor-bearing mice, only very small concentrations of the radiopharmaceuticals actually reached the interstitial fluid bathing the cancer cells. Under these conditions, the concentration of EGFRs on the breast cancer cells may have been in excess and the amount of radioligand would therefore be the limiting factor controlling tumor uptake. For example, based on a tumor uptake of ~2% ID/g (Fig. 1) and an injected dose of 1 μg ^{111}In-DTPA-hEGF, there would be $\sim 2 \times 10^{12}$ molecules of the radiopharmaceutical (0.02 μg) delivered to 2.5×10^8 MDA-MB-468 breast cancer cells contained in a 1 g breast cancer xenograft (assuming a breast cancer cell with a diameter of 20 μm). The cells would express a total of 2.5×10^{14} EGFR at an expression level of $\sim 10^6$ EGFR/cell (Table 1) and, therefore, there would be approximately a 100-fold excess of receptors present in the tumor compared with the radioligand. Similarly, for ^{111}In-DTPA-MAb 528, assuming an injected dose of 50 μg and a tumor uptake of 15 %ID/g (Fig. 1), there would be $\sim 3 \times 10^{13}$ molecules (7.5 μg) of MAb 528 delivered to the tumor. In this case, there would be a 10-fold excess of receptors compared with radioligand. The receptor level on the breast cancer cells was measured in vitro by increasing the concentration of radioligand until the concentration of receptors on the cells was the limiting factor. Under these conditions, breast cancer cells with a lower level of receptor expression (e.g., MCF-7 cells) bound less radioligand than cells with a higher level of receptor expression (e.g., MDA-MB-468 cells).

Although, the range of EGFR expression levels on the tumor xenografts studied was not as wide as that in this study, Rusckowski et al. (*31*) also noted a similar finding using ^{99m}Tc-EGF in athymic mice bearing either A431 squamous cell carcinoma or LS174T colon cancer xenografts. Despite a 6-fold difference in EGFR expression in vitro between the A431 and LS174T cells (2×10^6 versus 3.6×10^5 EGFR/cell, respectively), there was no statistically significant difference in tumor uptake in vivo (0.4 ± 0.09 versus 0.32 ± 0.06 %ID/g respectively). Senekowitsch-Schmidtke et al. (*35*) found a partial correlation between tumor uptake and EGFR level in human tumor xenografts implanted into athymic mice using ^{125}I-EGF but not with ^{125}I-labeled anti-EGFR MAb 425. The tumor uptake of ^{125}I-EGF was 2-fold higher in A431 xenografts compared with gastric cancer xenografts, but the A431 tumors expressed an 8-fold higher level of EGFRs. The tumor uptake of ^{125}I-MAb 425 was higher in breast cancer xenografts than in A431 tumors, despite higher EGFR expression by the A431 tumors. The results of this study suggest that the level of tumor localization of receptor-binding radiopharmaceuticals in vivo is controlled to a greater extent by their rate of elimination from the blood than by the level of receptor expression on cancer cells, provided that the radiopharmaceutical retains receptor-binding capability and a minimal level of receptors is available for binding. An analogous inverse correlation has also been observed previously between the elimination rate and tumor accumulation of different forms of radiolabeled MAbs (e.g., IgG versus $F(ab')_2$ versus Fab') (*25*).

CONCLUSION

The results of this study show that a direct quantitation of the level of receptor expression on cancer cells in vivo by γ scintigraphy may not be possible. Nevertheless, EGFR-positive tumor nodules in mice were detected qualitatively using radiopharmaceuticals that specifically bind to the receptor. Radiolabeled anti-EGFR MAbs would be more effective receptor-binding radiopharmaceuticals for tumor imaging in cancer patients than peptide-based agents, such as hEGF, because the slower elimination rate from the blood leads to higher tumor uptake at only moderately lower tumor-to-blood ratios. Clinical studies with ^{99m}Tc-anti-EGFR MAb ior egf/r3 have demonstrated that EGFR-positive lesions can be detected with high sensitivity in cancer patients (*36*).

ACKNOWLEDGMENTS

This research was supported in part by grants from DuPont Pharma, the Susan G. Komen Breast Cancer Foundation (grant no. 9749) and the U.S. Army Breast Cancer Research Program (grant no. DAMD17–98–1-8171) and by a grant from the National Cancer Institute of Canada with funds from the Canadian Cancer Society. Parts of this study were presented at the Society of Nuclear Medicine, 45th Annual Meeting, Toronto, Canada, on June 8, 1998.

REFERENCES

1. Klijn JGM, Berns PMJJ, Schmitz PIM, Foekens JA. The clinical significance of epidermal growth factor receptor (EGF-R) in human breast cancer: a review of 5232 patients. *Endocr Rev.* 1992;13:3–17.
2. Mendelsohn J. Epidermal growth factor receptor as a target for therapy with antireceptor monoclonal antibodies. *J Natl Cancer Inst Monogr.* 1992;13:125–131.
3. Fry DW, Kraker AJ, McMichael A, et al. A specific inhibitor of the epidermal growth factor receptor tyrosine kinase. *Science.* 1994;265:1093–1095.
4. Shaw JP, Akiyoshi DE, Arrigo DA, et al. Cytotoxic properties of DAB_{486}EGF and DAB_{389}EGF, EGF receptor targeted fusion toxins. *J Biol Chem.* 1991;266:21118–21124.
5. Reilly RM, Kiarash R, Cameron RG, et al. ^{111}In-labeled EGF is selectively radiotoxic to human breast cancer cells overexpressing EGFR. *J Nucl Med.* 2000;41:429–438.
6. Andersson A, Capala J, Carlsson J. Effects of EGF-dextran-tyrosine-^{131}I conjugates on the clonogenic survival of cultured glioma cells. *J Neuro Oncol.* 1992; 14:213–223.
7. Kuukasjarvi T, Kononen J, Helin H, Isola J. Loss of estrogen receptor in recurrent breast cancer is associated with poor response to endocrine therapy. *J Clin Oncol.* 1996;14:2584–2589.
8. Fischman AJ, Babich JW, Strauss HW. A ticket to ride: peptide radiopharmaceuticals. *J Nucl Med.* 1993;34:2253–2263.
9. Gill GN, Kawamoto T, Cochet C, et al. Monoclonal anti-epidermal growth factor receptor antibodies which are inhibitors of epidermal growth factor binding and antagonists of epidermal growth factor-stimulated tyrosine protein kinase activity. *J Biol Chem.* 1984;259:7755–7760.
10. Filmus J, Trent JM, Pollak MN, Buick RN. Epidermal growth factor receptor gene-amplified MDA-468 breast cancer cell line and its non-amplified variants. *Mol Cell Biol.* 1987;7:251–257.
11. Reilly RM, Gariépy J. Investigation of factors influencing the sensitivity of tumor detection using a receptor-binding radiopharmaceutical. *J Nucl Med.* 1998;39:1037–1042.
12. Reilly RM, Marks A, Law J, Lee NS, Houle S. In-vitro stability of EDTA and DTPA immunoconjugates of monoclonal antibody 2G3 labelled with In-111. *Appl Radiat Isot.* 1992;43:961–967.
13. Motulsky HJ, Stannard P, Neubig R. *Prism Ver 2.0* [software]. San Diego, CA: GraphPad Software Inc.; 1995.
14. Lindmo T, Boven E, Cuttitta F, Fedorko J, Bunn PA Jr. Determination of the immunoreactive fraction of radiolabelled monoclonal antibodies by linear extrapolation of binding to infinite antigen excess. *J Immunol Methods.* 1984;72:77–89.
15. Dunn WA, Hubbard AL. Receptor-mediated endocytosis of epidermal growth factor by hepatocytes in the perfused rat liver: ligand and receptor dynamics. *J Cell Biol.* 1984;98:2148–2159.
16. Gladhaug P, Christoffersen T. Kinetics of epidermal growth factor binding and processing in isolated intact rat hepatocytes: dynamic externalization of receptors during ligand internalization. *Eur J Biochem.* 1987;164:267–275.
17. Yanai S, Sugiyama Y, Kim DC, et al. Binding of human epidermal growth factor to tissue homogenates of the rat. *Chem Pharmacol Bull.* 1987;35:4891–4897.
18. Fisher DA, Salido EC, Barajas L. Epidermal growth factor and the kidney. *Annu Rev Physiol.* 1989;51:67–80.
19. St. Hilaire RJ, Hradek GT, Jones AL. Hepatic sequestration and biliary secretion of epidermal growth factor: evidence for a high-capacity uptake system. *Proc Natl Acad Sci USA.* 1983;80:3797–3801.
20. De Acosta CM, Justiz E, Skoog L, Lage A. Biodistribution of radioactive epidermal growth factor in normal and tumor bearing mice. *Anticancer Res.* 1989;9:87–92.
21. Scott-Robson S, Capala J, Carlsson J, et al. Distribution and stability in the rat of a ^{76}Br/^{125}I-labelled polypeptide, epidermal growth factor. *Nucl Med Biol.* 1991;18: 241–246.
22. Vinter-Jensen L, Frokiaer J, Jorgensen PE, et al. Tissue distribution of ^{131}I-labelled epidermal growth factor in the pig visualized by dynamic scintigraphy. *J Endocrinol.* 1995;144:5–12.
23. Tyson LM, Browne CA, Jenkin G, Thorburn GD. The fate and uptake of murine epidermal growth factor in the sheep. *J Endocrinol.* 1989;123:121–130.
24. Duncan JR, Welch MJ. Intracellular metabolism of indium-111-DTPA labeled receptor targeted proteins. *J Nucl Med.* 1993;34:1728–1738.
25. Reilly RM, Sandhu J, Alvarez-Diez T, et al. Problems of delivery of monoclonal antibodies: pharmaceutical and pharmacokinetic solutions. *Clin Pharmacokinet.* 1995;28:126–142.
26. Kim DC, Sugiyama Y, Fuwa T, et al. Kinetic analysis of the elimination process of human epidermal growth factor (hEGF) in rats. *Biochem Pharmacol.* 1989;38:241–249.
27. Jorgensen PE, Poulson SS, Nexo E. Distribution of intravenously administered epidermal growth factor in the rat. *Regulatory Peptides.* 1988;23:161–169.
28. Nielsen S, Nexo E, Christensen EI. Absorption of epidermal growth factor and insulin in rabbit renal proximal tubules. *Am J Physiol.* 1989;256:E55–E63.
29. Carpenter G, Cohen S. Epidermal growth factor. *Ann Rev Biochem.* 1979;48:193–216.
30. Capala J, Barth RF, Bailey MQ, Fenstermaker RA, Marek M, Rhodes, BA. Radiolabeling of epidermal growth factor with ^{99m}Tc and in vivo localization following intracerebral injection into normal and glioma-bearing rats. *Bioconjug Chem.* 1997;8:289–295.
31. Rusckowski M, Qu T, Chang F, Hnatowich DJ. Technetium-99m labeled epidermal growth factor-tumor imaging in mice. *J Peptide Res.* 1997;50:393–401.
32. Cuartero-Plaza A, Martinez-Miralles E, Rosell R, Vadell-Nadal C, Farre M, Real FX. Radiolocalization of squamous lung carcinoma with ^{131}I-labeled epidermal growth factor. *Clin Cancer Res.* 1996;2:13–20.
33. Goldenberg A, Masui H, Divgi C, et al. Imaging of human tumor xenografts with an indium-111-labeled anti-epidermal growth factor receptor monoclonal antibody. *J Natl Cancer Inst.* 1989;81:1616–1625.
34. Divgi CR, Welt S, Kris M. Phase I and imaging trial of indium-111 labeled anti-EGF receptor monoclonal antibody 225 in patients with squamous cell lung carcinoma. *J Natl Cancer Inst.* 1991;83:97–104.
35. Senekowitsch-Schmidtke R, Steiner K, Haunschild J, Mollenstadt S, Truckenbrodt R. In vivo evaluation of epidermal growth factor (EGF) receptor density on human tumor xenografts using radiolabeled EGF and anti-(EGF receptor) mAb 425. *Cancer Immunol Immunother.* 1996;42:108–114.
36. Ramos-Suzarte M, Rodríguez N, Oliva JP, et al. ^{99m}Tc-labeled antihuman epidermal growth factor receptor antibody in patients with tumors of epithelial origin: part III. Clinical trials safety and diagnostic efficacy. *J Nucl Med.* 1999;40:768–775.

heated with $(But)_4NF$ in EtOAC at 70°C for 20 min. The *arabino* fluorosugar was characterized by spectroscopic methods (NMR and MS). Radiochemical syntheses were performed with F-18 fluoride. F-18 fluoride was reacted with $(But)_4NHCO_3$ and evaporated to dryness. The dry $(But)_4NF$ was dissolved in THF and heated with the 2-O-fluorosulfonyl derivative in EtOAc. The crude product was purified by HPLC. **Results:** The average radiochemical yield was 19% in 11 runs, with radiochemical purity >99%. Specific activities were 4.4-9.3 GBq/μmole. Synthesis time was 75-80 min from EOB. **Conclusion:** The arabinofuranose was successfully labeled with F-18 and may be a useful intermediate for synthesis of nucleoside analogues for PET.

No. 1369

TUMOR LOCALIZATION OF TC-99M LABELED 5-THIO-D-GLUCOSE (TG).

K. S. Ozker*, B. D. Collier, D. J. Lindner, A. Z. Krasnow, R. S. Hellman, Y. Liu, L. Kabasakal, D. S. Edwards, C. R. Bourque, P. D. Crane, Medical College of Wisconsin, Milwaukee, WI; University of Maryland, Baltimore, MD; Cerrahpasa Medical School, Istanbul, Turkey; DuPont Merck Pharmaceutical Company, North Billerica, MA. (101093)

Objectives. Recent studies attest to the avididty of Tc-99m labeled carbohydrate ligands (glucarate and gluconate) for tumors and sites of acute ischemic injury. The exact mechanism of localization for Tc-99m labeled carbohydrate ligands is currently not known. The purpose of this work is to study the pattern of tumor localization of a Tc-99m labeled carbohydrate ligand, Tc-99m-TG. TG, an analog of D-glucose, binds to Tc-99m via a thio substitute. **Methods.** Biodistribution studies of Tc-99m-TG administered to mice bearing MC26 colon carcinoma in their thigh was used to determine the tumor localization and tumor to BG (normal muscle from contralateral thigh) ratios. Autoradiography of Tc-99m-TG was also compared to that of C-14 labeled 2-deoxyglucose (C-14-DG) in a subgroup of mice. **Results.** Tumor uptake of Tc-99m-TG was 1.6 ± 0.3% ID/g at 1 hour which decreased slightly to 1.3 ± 0.3% ID/g and 1.2 ± 0.3% ID/g at 2 and 3 hours post-injection respectively. However, tumor to BG ratio exhibited a significant increase between 1 and 3 hours (2.7/1 and 4/1), due to gradually decreasing body BG. Tumor autoradiography of Tc-99m-TG and C-14-DG showed different patterns of localization. Tc-99m-TG concentrated at the center of the tumors while C-14-DG had decreased activity in this central area, suggesting Tc-99m-TG avidity to zones of infarction/necrosis and C-14-DG avidity to viable tumor cells in the periphery. **Conclusion.** Results of this study indicate that Tc-99m-TG exhibits increased tumor localization and T/BG ratio. The discordance between tumor localization of Tc-99m-TG and C-14-DG suggests that Tc-99m-TG does not act like a glucose analog and warrants further investigation as an imaging agent for areas of necrosis.

No. 1370

PRODUCTION OF A HUMAN EPIDERMAL GROWTH FACTOR (HEGF)-IMMUNOGLOBULIN (C_H1)FUSION PROTEIN FOR TARGETING HUMAN BREAST CANCER.

J. Wang*, J. Sandhu, Z. Chen, C. Leung, M. Bray, S. Yang, R. Cameron, A. Hendler, K. Vallis, R. M. Reilly, The Toronto Hospital, Toronto, ON, Canada; Samuel Lunenfeld Research Institute, Toronto, ON, Canada; Ontario Cancer Institute, Toronto, ON, Canada; Princess Margaret Hospital, Toronto, ON, Canada; The Toronto Hospital/University of Toronto, Toronto, ON, Canada. (100173)

Overexpression of the EGF receptor (EGFR) occurs in 30-60% of breast cancers. Preliminary studies showed that In-111 hEGF localized specifically in MDA-468 human breast cancer xenografts ($>10^6$ EGFR/cell)in nude mice (tumour/blood ratio >12: 1) but tumour uptake was low (2-3 % i.d./g). Tumour uptake of hEGF (m.w. 6 kDa) could possibly be improved by slowing its renal elimination by fusion with a macromolecule. **Objective:** To produce an hEGF fusion protein consisting of hEGF and the C_H1 domain of IgG_1 to more effectively target radionuclides to EGFR-positive breast cancer. **Methods:** The gene for hEGF (*pADH59*) was fused with the gene for C_H1 of $mIgG_1$ (*pASK84*) with/without a peptide linker sequence $[(GGGGS)_3]$ and inserted into expression vector *pGEX2T*. E.coli (BL21) were transformed with the *p-hEGF-C_H1* expression vector and ampicillin-resistant colonies grown to produce a hEGF-C_H1 glutathione S-transferase (GST) fusion protein. GST-hEGF-C_H1 protein was extracted under native conditions and purified on a glutathione-Sepharose column. GST-hEGF-C_H1 was assessed for purity by SDS-PAGE and Western blot with a polyclonal anti-EGF antibody and for receptor binding by ELISA and flow cytometry. **Results:** GST-hEGF-C_H1 protein was obtained in high yield (1 mg/L). SDS-PAGE showed a single band (m.w. 44 kDa) positive for hEGF by Western blot. GST-hEGF-C_H1 exhibited strong binding by ELISA to EGFR isolated from MDA-468 breast cancer cells and to live A431 cells by flow cytometry. **Conclusion:** An hEGF-C_H1 fusion protein with preserved receptor-binding properties was produced in high yield and purity. Experiments are planned to evaluate the hEGF-C_H1 protein labelled with In-111 for targeting MDA-468 breast cancer xenografts in nude mice. Supported by Susan G. Komen Breast Cancer Foundation and US Army BCRP.

No. 1371

ENHANCED ACCUMULATION OF ALBUMIN IN INTRAPERITONEAL TUMORS FOLLOWING MANNOSYLATION.

Z. Yao*, M. Zhang, H. Sakahara, Y. Arano, H. Saji, J. Konishi, Clinical Center, The National Institutes of Health, Bethesda, MD; Kyoto University, Kyoto, Japan. (500312)

We have shown that glycosylation of avidin is one of the important factors of its tumor accumulation. This study was undertaken to investigate the potential of glycosylated albumin in targeting intraperitoneal (i.p.) tumor xenografts. Three tumor xenograft models, including a colon cancer, LS180, an ovarian cancer, SHIN-3, and a gastric cancer, MKN45, were established by i.p. injections of the human cancer cells in nude mice. Human serum albumin (HSA) was conjugated with galactose or mannose. Galactosyl-neoglycoalbumin (NGA), mannosyl-neoglycoalbumin (NMA), or HSA was labeled with In-111 through SCN-Bz-EDTA conjugation. The radiolabeled proteins were administered i.p. into the tumor-bearing mice and the biodistribution of radioactivity was examined at 2 and 24 hours postinjection. The results show that glycosylation of albumin increased blood clearance and liver accumulation of radioactivity. Tumor uptake was significantly increased with NMA, resulting in a high tumor-blood ratio. NGA accumulated in tumors higher than HSA but much lower than NMA. Similar biodistribution pattern of radioactivity was also observed 24 hour postinjection. The biodistribution in SHIN-3 or MKN45 tumor-bearing mice was similar to that in LS180. In conclusion, mannosyl glycosylation of albumin enhanced its accumulation in i.p. tumors when administered i.p.. The high targeting efficiency could make NMA a useful vehicle for the delivery of radionuclide or other therapeutic agents to i.p. tumors for the diagnosis and therapy.

Biodistribution of radioactivity in mice bearing LS180 xenograft (%ID/g, 2 h)

	HSA	NGA	NMA
Blood	8.50±2.75	0.28±0.23	0.30±0.08
Liver	2.97±0.75	18.31±6.49	12.95±2.98
Tumor	3.61±0.75	6.17±1.12	19.31±4.07

No. 1372

SYNTHESIS AND CHARACTERISATION OF I-123- AND I-125-DIETHYLSTILBESTROL (DES) WITH HIGH SPECIFIC ACTIVITY.

K. Schomaecker, T. Fischer*, H. Schmickler, B. Meller, B. Gabruk-Szostak, H. Schicha, Clinic of Nuclear Medicine, University of Cologne, Cologne, Germany; University of Cologne/Institute of Organic Chemistry, Cologne, Germany; Department of Nuclear Medicine, University of Luebeck, Luebeck, Germany. (100073)

Rationale: Radioactive labeled DES is an interesting compound for therapy of estrogen receptor (ER)- positive mamma-carcinoma. Until now, labeling procedures suffered from low yields (20 - 30%) with low specific activities (0.74 - 2.96 GBq/mmol) and bad reproducibility. Aims: a) Development of a simple and fast labeling method for *I-DES with high yield and specific activity b) Structure analysis by NMR c) Determination of the dissociation constant. **Methods:** a) Labeling was done with chloramine T in methanol within 10 min at room temperature. Purification was performed with RP-HPLC. For NMR experiments, synthesis was done with stable iodine, followed by preparative HPLC. b) For structure analysis ^{1}H-NMR, ^{13}C-NMR, H,H-COSY and HMBC were used. c) Dissociation constant was determined by incubation of ER-positive tumor cytosol with varied ^{125}I-DES amounts, with and without additional DES, followed by a Scatchard plot. **Results:** a) *I-DES was produced with yields of 50 - 70% and specific activity of 80 TBq/mmol. b) Some of the reaction products could be identified and the structure of I-DES was verified. 3-iodo-DES and 2-iodo-DES were found in a 8.5/1 ratio. c) The dissociation con-